ON THE PREDICTABILITY OF TIME SERIES BY METRIC ENTROPY

A Thesis Submitted to
the Graduate School of Engineering and Sciences of
İzmir Institute of Technology
in Partial Fulfillment of the Requirements for the Degree of

MASTER OF SCIENCE

in Mechanical Engineering

by
Hakkı Erhan SEVİL

July, 2006
İZMİR

We approve the thesis of **Hakkı Erhan SEVİL**

                                                                    Date of Signature

…………………………   **12 July 2006**
Asst. Prof. Dr. Serhan ÖZDEMİR
Supervisor
Department of Mechanical Engineering
İzmir Institute of Technology

……………………………   **12 July 2006**
Prof. Dr. Ferit Acar SAVACI
Department of Electrical and Electronics Engineering
İzmir Institute of Technology

……………………………   **12 July 2006**
Asst.Prof. Dr. Şevket GÜMÜŞTEKİN
Department of Electrical and Electronics Engineering
İzmir Institute of Technology

…………………………   **12 July 2006**
Assoc. Prof. Dr. Barış ÖZERDEM
Head of Department
İzmir Institute of Technology

                                 …………………………
                          Assoc. Prof. Dr. Semahat ÖZDEMİR
                              Head of the Graduate School

..and the future is certain..
...give use to work it out…[*]

ACKNOWLEDGMENTS

ABSTRACT

ON THE PREDICTABILITY OF TIME SERIES BY METRIC ENTROPY

The computation of the metric entropy, a measure of the loss of information along the attractor, from experimental time series is the main objective of this study. In this study, replacing the current warning systems (simple threshold based, on/off circuits), a new and promising prognosis system is tried to be achieved by the metric entropy, i.e. Kolmogorov – Sinai entropy, from chaotic time series. Additional to metric entropy, correlation dimension and time series statistical parameters were investigated. Condition monitoring of ball bearings and drill bits was achieved in the light of practical considerations of time series applications. Two different accelerated bearing run-to-failure test rigs were constructed and the prediction tests were performed. However, as a reason of shaft failure in both structures during the experiments, none of them is completed. Finally, drill bit breakage experiments were carried out. In the experiments, 10 small drill bits ($1 \ mm\phi$) were tested until they broke down, while vibration data were consecutively taken in equal time intervals. After the analysis, a consistent decrement in variation of metric entropy just before the breakage was observed. As a result of the experiment results, metric entropy variation could be proposed as an early warning system.

ÖZET

ZAMAN SERİLERİNİN METRİK ENTROPİ YARDIMIYLA TAHMİN EDİLEBİLİRLİĞİ

Bu çalışmanın birincil amacı, deneysel zaman serilerinde, çekici boyunca bilgi kaybına eşit olan metric entropinin hesaplanmasıdır. Bu çalışmada, varolan basit eşik değerine dayanan uyarı sistemleri yerine, kaotik zaman serilerinden metrik entropi ile, diğer adıyla Kolmogorov-Sinai entropi ile, yeni ve umut verici bir hata teşhis sistemi başarılmaya çalışılmıştır. Zaman serilerinin pratik kullanımı ışığında, rulman ve matkap ucu durum izlemeleri gerçekleştirilmiştir. İki farklı hızlandırılmış rulman kırma test düzeneği ve testleri yapılmıştır. Fakat, iki düzenekte de deney sırasında şaft kırılmaları sonucu, testler tamamlanamamıştır. Son olarak, matkap ucu kırılma deneyleri yapılmıştır. Deneylerde, 10 adet küçük matkap ucu ($1\,\mathrm{mm}\,\phi$) kırılana kadar test edilmiş ve eşit aralıklı ardışık titreşim verileri alınmıştır. Analizler sonunda, metrik entropi değişiminde, kırılmadan az önce, tutarlı bir düşme gözlenmiştir. Deneylerin sonucunda, metrik entropi değişimi erken uyarı sistemi olarak önerilebilir.

TABLE OF CONTENTS

LIST OF FIGURES

LIST OF TABLES

CHAPTER 1

INTRODUCTION

Time series analysis comprises methods that attempt often either to understand the underlying theory of the data points or to make forecasts of time series, which are sequence of data points, measured typically at successive times spaced apart at uniform time intervals. The last decade has brought dramatic changes in the way that researchers analyze time series. Nonlinear time series analysis is becoming more and more reliable tool for the study of complicated dynamics from measurements.

Most real-world systems are nonlinear and can be analyzed by nonlinear techniques (Buzug 1994). Caputo et al. manage to analyze dynamic behavior of fluidized bed systems from some selected time series data. The most impressive feature of the nonlinear dynamics is chaos theory. Chaos is an aperiodic long-term behavior of a bounded, deterministic system that has sensitive dependence on initial conditions, where this feature is popularly known as "butterfly effect".

Due to the fact that nearly all the observable phenomena in daily lives or in scientific investigation are nonlinear, the importance of nonlinear dynamics is increasing day by day. Chaos and nonlinear dynamics have provided new theoretical and conceptual tools which allow comprehending the complex behaviours of systems. Being a developing tool, through out the literature, various solutions are achieved by the usage of these tools. Mechanical systems with backlash components were quantified by the chaotic behaviour of the responses and correlation between the quantification parameters and the parameters of the (non-linear) system is obtained (Tjahjowidodo et al. 2005). Elshorbagy et al. (2002) analyzed time series in means of nonlinear techniques for the estimation of missing stream flow data. After the chaotic behavior in the daily flows of the river is investigated, the reconstructing of phase space of a time series is utilized to identify the characteristics of the non linear dynamics.

In the literature on dynamical systems and chaos, the terms *phase space* and *state space* are often used interchangeably. Phase space is a mathematical space which is completely filled with trajectories, since each point can serve as an initial condition.

At any instant time the state of system can be completely specified by indicating a point in state space.

Correlation dimension is a characteristic quantity for time series and has been continuously gaining popularity by means of quantifying chaotic time series data. Determination of the correlation dimension from experimental chaotic time series data involves two steps. First, reconstruction of the phase space, then the computation of the correlation dimension from the phase space vectors. The condition monitoring of bearing systems with the effect of the gap clearance were characterized by the application of embedding space and correlation dimension estimation (Craig et al. 2000). Furthermore, experimental results from a rolling element bearing from experiment rig are successfully diagnosed by using correlation dimension. With correlation dimension value, healthy and defected bearings were indicated. Also, defect type classification was achieved (Logan 1995).

Chen et al. (1998) used the short term predictability feature of the chaotic systems and phase space characterization to make one-hour to one-day predictions of ozone levels. A reconstructed phase space model was applied to atmospheric environment and used for the ozone levels prediction. The predictability of time series can be indicated by metric entropy which is a measure of the rate of loss of predictability. Metric entropy (as known as Kolmogorov – Sinai Entropy) obtains that how far the future can be predicted with a given initial information. Drongelen et al. (2003) demonstrated the feasibility of using analysis of the Metric Entropy of the time series to anticipate seizures in pediatric patients with intractable epilepsy. Anticipation times varied between 2 and 40 minutes.

Although most of the observable dynamical systems are nonlinear, before applying nonlinear techniques, it is necessary to first ask, if the use of such advanced techniques is justified by the data. Nonlinearity test with surrogate data is a process that indicates the existence of the nonlinearity in the system (Schreiber 2001).

Another topic in nonlinear time series analysis is the effect of noise. Hegger et al. (1999) proposed a simple nonlinear noise reduction for the analysis of observed chaotic data. On the other hand, Elshorbagy et al. (2002) showed that the used of that algotrithm for noise reduction might remove significant part of the original signal and introduce nonexisting chaotic behaviour.

Condition monitoring of a machine can be thought as a decision support tool which is able to indicate the development of probable failure in machinery component

or system, and that also predict failure occurrence. Even so, condition monitoring allows avoidable actions which performed before a failure happened. The most commonly used method for condition monitoring is vibration analysis. Although there are different types of condition monitoring techniques currently in use for the diagnosis and prediction of machinery faults, little attention has been paid to the detection of chaotic behaviour in time series vibration signal. The field of condition monitoring is always open to the introduction of new techniques for machine fault diagnosis. Therefore comparisons can be drawn between combinations of several different diagnosis techniques. Monitoring of a machining process is done by Govekar et al. (2000) on the basis of sensor signal analysis. For signal analysis, methods of nonlinear time series analysis are used. In recent years time series characterization is started to be utilized as a condition monitoring and fault detection tool. Current fault detection systems are simple threshold-based on-off circuits. The threshold values are determined by experiments and set with an appropriate safety margin. These safety limits govern the running of the machines, or human heart, and once set, they are not supposed to change in time. In reality, these systems are not even needed. Since, no time or financial losses might be spared when it is too late. For instance, on an assembly line, to predict the failure of a failure-prone part within the work hours even before it has failed, and replace it might prevent the whole line from squandering precious hours on idle. Moreover on a vehicle, monitoring of a critical component real-time and on-line, and maintaining a view of the part could save lives, and months-long litigations in court for the manufacturers. Furthermore, a classification based method for condition monitoring of robot joints using non-linear dynamics characteristics was proposed by Trendafilova et al. (2000).

In the condition monitoring field, on-line tool condition monitoring has a great significance in modern manufacturing processes. Sensing techniques, which have high reliability, have been developed for providing a rapid response to an unexpected tool breakage to prevent possible damages to the workpiece and machine component. Also, several techniques on the detection of tool breakage for monitoring the drilling processes have been developed over the past years (Xiaoli 1999 and Mori et al. 1999).

This study attempts to correlate the chaos invariants with the changing conditions of a drilling process. Also, prediction of small drill bit breakage was examined by using metric entropy. Briefly, the aim of this study is to introduce a possible early damage detection method for mechanical systems.

This study presents experimental and a detailed analysis of mechanical drilling system which shows chaotic behaviour. The computation of the invariants was carried out by the TISEAN package (Hegger et al. 1999). In addition to that, various MatLAB codes and time series analysing program *Culpertus* (Appendix C) were created.

CHAPTER 2

TIME SERIES ANALYSIS

Time series analysis comprises methods that attempt to understand the data generating mechanism(s) of time series which are sequence of data points, measured typically at successive times, spaced apart at uniform time intervals. There are two main aims of time series analysis: (i) identifying the underlying theory of the phenomenon represented by the data points, and (ii) making forecasts (predicting future values of the time series variable). Both aims require the analyze of observed data point. Due to the fact that the nonlinear dynamics of time series can produce chaotic time series, previous data points are analized by nonlinear techniques.

2.1. Nonlinear Dynamics

The term dynamic refers to phenomena that produce time changing patterns, where the characteristics of which at one time is interrelated with those at past times. The dynamic of any situation refers to how the situation changes over the course of time. A dynamical system is a physical setting together with rules for how the setting changes or evolves from one moment of time to the next. Dynamical systems can be either stochastic where the system evolve with respect to some random processes such as the toss of coin, or deterministic where the future uniquely determined by the past times.

Nonlinear systems represent systems whose behavior is not expressible as a sum of the behaviors of its descriptors. In particular, the behavior of nonlinear systems is not subject to the principle of superposition, as linear systems are. In nonlinear systems, a small change in a parameter can lead to sudden and dramatic changes in both qualitative and quantitative behavior of the system. As a result of this sensitivity, the behavior of systems that exhibit chaos appears to be random, even though the system is deterministic. The importance of nonlinear dynamics leans on the fact that nearly all the observable phenomena in daily lives or in scientific investigation are nonlinear.

2.2. Characteristics of Chaotic Behavior

In mathematics and physics, although there is no universally accepted definition of chaos, it is defined as "Stochastic behavior occurring in a deterministic system". The most important feature of chaos is the unpredictability of the future although it is a deterministic system. Deterministic chaos refers to irregular or chaotic motion that is generated by nonlinear systems evolving according to dynamical laws that uniquely determine the state of the system at all times from a knowledge of the system's previous history. It is important to point out that the chaotic behavior is due neither to external sources of noise nor to an infinite number of degrees-of-freedom nor to quantum-mechanical-like uncertainty. As a property of chaos, some sudden and dramatic changes in systems may give rise to the complex behavior. Briefly, chaos is an aperiodic long-term behavior of a deterministic system that has sensitive dependence on initial conditions. The irregular behavior of chaotic system comes from the system's nonlinearity, although it has no random inputs or parameters as a deterministic system. Also, as mentioned above, chaos is a long-term behavior, which means that in a chaotic system, the trajectories do not settle down to a limit cycle, a fixed point, a periodic orbit etc. A practical implication of chaos is that its presence makes it essentially impossible to make any longterm predictions about the behavior of a dynamical system.

A chaotic dynamical system must satisfy the following requirements;

- The periodic orbits of the system must be dense,
- The system must be transitive,
- The system must be sensitive to initial conditions.

The density of periodic orbits in phase space is satisfied that for any point x in phase space, any neighborhood of x contains at least a point from periodic orbits. Furthermore, the transitivity means that no matter where the initial position on the attractor, the dynamics' trajectory will be arbitrarily close to every other point on the attractor.

The most striking and the most known property of chaotic systems is the sensitive dependence to initial conditions. Also it is popularly known as the "butterfly effect". This property can be described simply as, exponential separation of the nearby

trajectories. even the difference of two initial positions is very small, that two points in a chaotic system may move in extensively different trajectories, like flapping of a butterfly's wings might create cause a tornado to occur over time. Only if the initial conditions of two points are exactly the same, the system gives the same identical results. In addition to that, for all chaotic systems, the trajectory of the system never repeats.

2.3. Phase Space Representation

Phase space is a mathematical space spanned by the dependent variables of a given dynamical system and in that space; all possible states of that system are represented. In other words, phase space is a representor of a dynamical system where each point on that phase space represents a particular state of the system at a particular time (Figure 2.1).
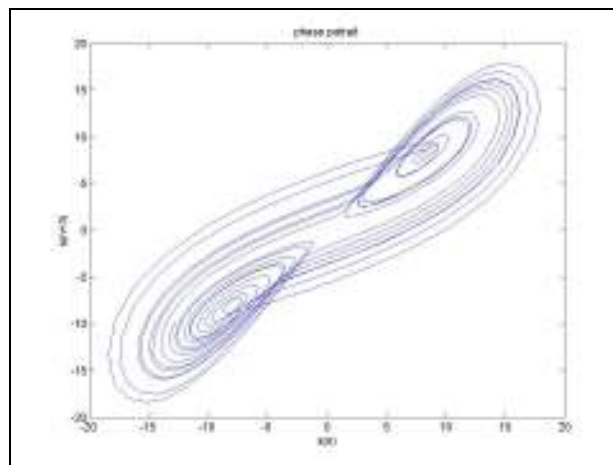
Figure 2.1. Phase Space Representation of Lorenz System

Phase Space representation is versatile tool in time series analysis. Due to the fact that, phase space determine all the states of a dynamical system, analysis of that system can be achieved in both identifying the system and predicting the future states via phase space representation. Because of phase space method is such a powerful technique; so many algorithms depend on phase space representation exist. From time series point of view, phase space representation is very useful, too. Although the actual phase space (state space) is unknown in experimental one dimensional time series, as a

substitute, an embedded phase space can be reconstructed by delay reconstruction technique. In that embedded phase space, the phase space analysis can be applied because embedded phase space own the same geometric properties as the state space. This fact arises from the fact that the attractor in reconstructed phase space is one-to-one image of the attractor in state space.

2.3.1. Attractor Geometry

The strange behavior of chaotic systems has geometry of the set in phase space formed by the trajectories of the system called the attractor which the trajectories in phase space will have some final state on it, as the system evolves in time. Briefly, an attractor is a set to which all neighboring trajectories converge. Moreover, the attractor of a system determines the long-term behavior of that system. Basin of attraction for an attractor is a set of initial positions which are giving rise to trajectories that approach to a given attractor. Attractors are generally called as *strange attractors*, due to the fact that they generally have a very complicated geometry, fractal (self similarity) structure, in chaotic systems.

Strange attractors have some characteristic features, i.e. any orbit or trajectory that starts on them stays on them for all time. Also, they have usually a noninteger dimension which is less than the dimension of phase space, e.g. if the phase space is two dimensional, the attractor will have a dimension less than two.

2.3.2. Reconstruction of Phase Space

Physical phase space is the most important problem in time series analysis due to the fact that it is unknown. As a result, the computations are made in some alternative space called embedded or reconstructed space. The embedded (reconstructed) space enables to draw out a multidimensional description of state space dynamics from the time series data of a single dynamical variable, and generalizes the quantitative measures of chaotic behavior.

Behavior of trajectories has the same geometric and dynamical properties in the properly constructed embedding space. Geometric and dynamical properties characterize the actual trajectories in the full multidimensional state space for the

system. The behavior of the actual trajectories in the full state space is mimicked by the trajectories in the embedding space.

Firstly, in 1980, Packard, Crutchfield, Farmer and Shaw suggested the theory of generating a reconstruction space from a single time series to characterize nonlinear dynamical systems, and the theory was completed by F.Takens. In 1981, he proved that the time-delayed variables constitute an adequate embedding provided the measured variable is smooth and couples to all the other variables.

2.3.2.1 Delay Reconstruction

The time-delayed embedding space is reconstructed state space chosen with the minimum dimension for which the important dynamical and topological properties are maintained. For most purpose this dimension need only be the next integer larger than $2D_A$, where D_A is the attractor dimension. The reconstructed attractor is a one-to-one image of the attractor in the original phase space, and this is the requirement of the minimal sufficient embedding dimension "m".

$$\mathbf{s}_n = \left(s_n, s_{n-v}, \ldots, s_{n-(m-2)v}, s_{n-(m-1)v} \right) \tag{2.1}$$

In this study, the time series analyses are processed as discrete time systems. Therefore, replacing to the time lag τ for continuous systems, the sample lag v is used. The relation between these two is; $\tau = v \Delta t$, where Δt is the sampling interval of the data.

Computationally, finding optimum value m takes few steps to the result. At the beginning, although the optimal embedding dimension is unknown, embedding phase space can be reconstructed for various values of m with using optimum time lag v, e.g. for $m=2,3,\ldots 7$.

For reconstructing a embedding vector $\mathbf{s}_n$, first, the sample s_n is taken into the vector, and then v lagged sample s_{n+v}, $2v$ lagged sample s_{n+2v}, $3v$ lagged sample s_{n+3v} are added into the vector. The number of lagged samples which are added into the vector is denoted by phase space dimension number m.

During the formulation of reconstruction of phase space vector, for m values, the notation which varies between 0 to (m-1) is used. The reason of these is that every

vector $\mathbf{s}_n$ has its own sample s_n first (m=0). This notation of m values doesn't effect the dimension, because from 0 to (m-1) there are m pieces.

For the computational ease, the v next samples are added to the embedding vector. The lag direction of the embedding vectors doesn't make any difference. The formula can be created with adding the v previous samples or v next samples.

$$\mathbf{s}_n = (s_n, s_{n+v}, ..., s_{n+(m-2)v}, s_{n+(m-1)v}) \tag{2.2}$$

Table 2.1. Illustration of reconstructing of phase space

Phase Space Vector	Reconstructed Phase Space Dimension				
	1	2	...	m-1	m
$\mathbf{s_1}$=	s_1	s_{1+v}	...	$s_{1+(m-2)v}$	$s_{1+(m-1)v}$
$\mathbf{s_2}$=	s_2	s_{2+v}	...	$s_{2+(m-2)v}$	$s_{2+(m-1)v}$
⋮	⋮	⋮	...	⋮	⋮
$\mathbf{s_n}$=	s_n	s_{n+v}	...	$s_{n+(m-2)v}$	$s_{n+(m-1)v}$
⋮	⋮	⋮	...	⋮	⋮
$\mathbf{s_{N-(m-1)v}}$=	$s_{N-(m-1)v}$	$s_{N-(m-2)v}$	...	s_{N-v}	s_N

The value of v needs computational process. Basically, this value represent the inter relations between data samples. To find the optimum value of sample lag, either autocorrelation which is linear correlation of a time series with its own past or mutual information which is the probability about the value of s_{n+v} when the value of s_n is known, is used.

2.3.2.1.1. Autocorrelation

The time evolution of a system can be analyzed by using the autocorrelation of a signal. Autocorrelation measures how strongly on average each data point is correlated with one time step away. It is the ratio of the autocovariance to the variance of the data. Autocorrelation is a linear measure, each term of which measures the extent to which s_n versus s_{n+v} is a straight line. The autocorrelation of a time series is;

$$c_v = \frac{\frac{1}{N}\sum_{n=1}^{N}\{(s_n - \mu)(s_{n+v} - \mu)\}}{\sigma^2} \tag{2.3}$$

where μ is the mean value and the σ^2 is the variance value of the time series.

In general the autocorrelation function falls from 1 at $v=0$ to 0 at large values of v. In deterministic chaotic systems, the autocorrelation of the time series exponentially decreases with increasing lag values, thus the value v at which it falls exponentially is called the optimum correlation time. In implementation, firstly the c_v values are computed, with changing values of v in between 0 and ∞. The v value which first makes $c_v \approx 0$ or the decay of c_v exponentially is accepted as optimal lag (Figure 2.2). It is clear by the equation that the aim is to find the samples that are highly correlated each other with lag v. It should be noted that for a zero lag, autocorrelation equals to one.

2.3.2.1.2. Average Mutual Information

Mutual information is a tool to measures of independence between data samples. Unlike the autocorrelation function which is based on linear statistics, the mutual information takes into account also nonlinear correlations.
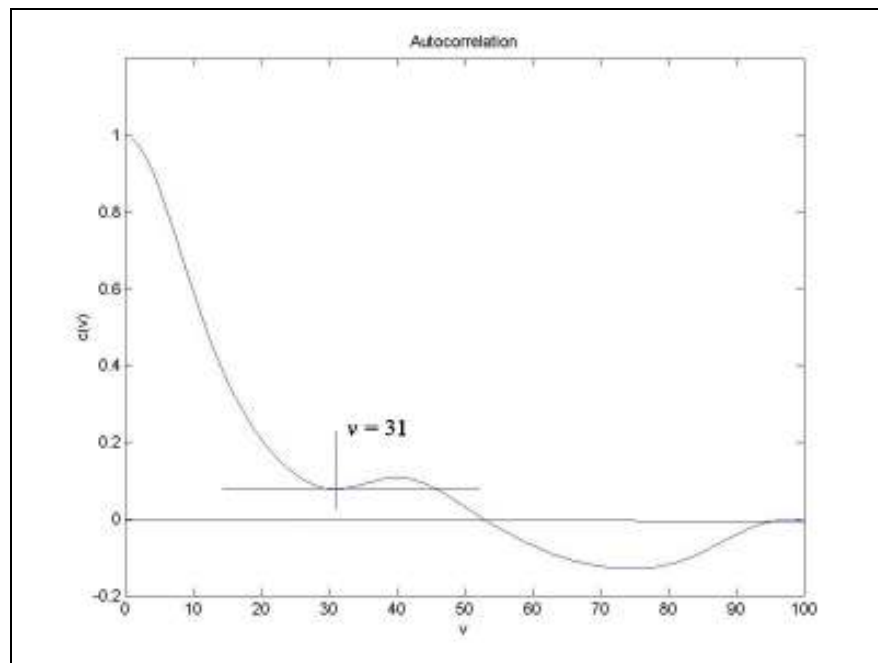
Figure 2.2. Autocorrelation of Lorenz System

Mutual information is simply gives probability about the value of s_{n+v}, when the value of s_n is known. The computation of mutual information is;

$$I(v) = \sum_{i,j} p_{ij}(v) \ln(p_{ij}(v)) - 2 \sum_{i} p_i \ln(p_i) \tag{2.4}$$

First of all, from the time series data, a histogram is created including various bins. The choice of the length of the bins (ε) is not important, as long as it is fine enough. As in the equation, p_i denotes the probability of s_n being in the ith bin of the histogram. Also p_{ij} denotes the probability of s_{n+v} being in j[th] bin while s_n is in the ith bin of the histogram. From the equation, the first minimum of the mutual information with related lag, $I(v)$, indicates the optimum sample lag where s_{n+v} adds maximum information to the knowledge which is gotten from s_n (Figure 2.3).
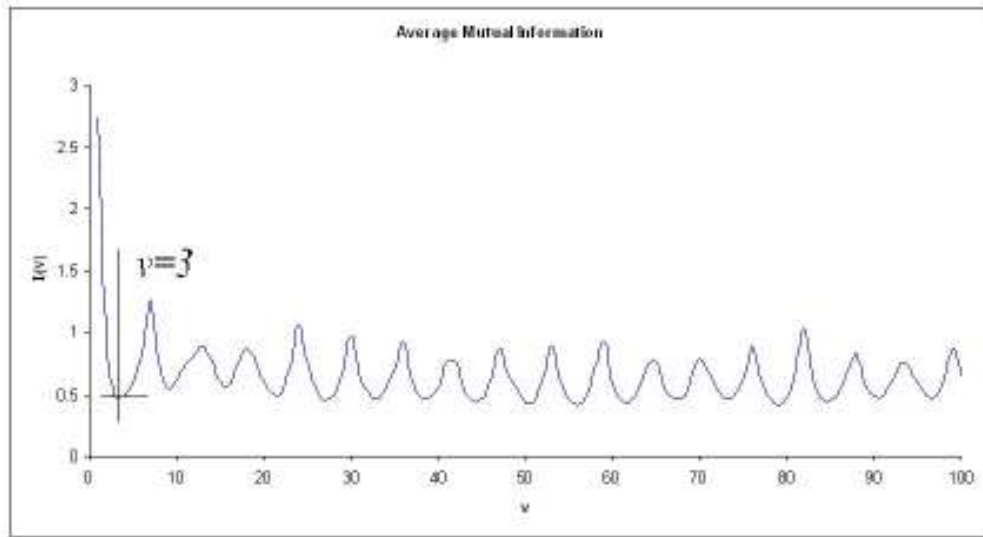
Figure 2.3. The average mutual information of Rössler System

2.3.2.2. Poincaré Sections

Poincaré section is a method for indicating the structure of a flow in a phase space more than two dimensions. Poincaré section is created by choosing a plane on the trajectory and recording on that plane the points at which the trajectory intersects that surface in a specified direction (same side of the plane). The intersection points give information about the dynamical system's behavior.

The choice of the poincaré section is not dependent on a rule. It need not be perpendicular to the trajectory, but it must not be tangent to trajectory. However, for better results, the placement of the plane must satisfied that it maximizes the number of

intersections with minimizes the time intervals between them. Depending to choice of the section and the path in the reconstructed phase space, the intersection points will vary. This method reduces the dimension of the attractor by one.

2.4. Chaotic Invariants

In experimental time series analyses, the chaotic invariants are used to determine the system condition, to making estimations and even predictions. In this study, invariants such as correlation dimension (a measure of the complexity that quantifies the geometry and shape of strange attractors), Lyapunov exponents (a measure of sensitivity of the process to initial conditions) and metric entropy (a measure of the loss of information along the attractor) are taken to consideration for time series analyses. Calculation of these invariants requires that the time series must be reconstructed into a embedded phase space.

2.4.1. Correlation Dimension

Correlation dimension is a measure of the fractal dimension of the time series, which measures the complexity that quantifies the geometry and shape of strange attractor. The correlation sum is used to estimate the correlation dimension.

2.4.1.1. Correlation Sum

In chaos theory the correlation sum is the estimator of the correlation dimension. The correlation sum for a collection of points $\mathbf{s}_n$ in some vector space is the fraction of all possible pairs of points which are closer than a given distance "epsilon" (ε) in a particular norm. The method of correlation sum consists of centering a hyper sphere on a point in hyper-space or phase space, letting the radius of the hyper sphere grow until all points are enclosed, and keeping track of the number of data points that are enclosed by the hyper sphere (Figure 2.4).

Correlation sum $C(\varepsilon)$ is the number of points within all the circles of radius ε (Figure 2.5). Similarly, correlation sum can be considered as the fact where the

probability of two different randomly chosen points will be closer than the distance ε. It is expected that $C(0)=0$ for a chaotic system due to the fact that the points never repeat in a non periodic system embedded without false nearest neighbor. The correlation sum of a time series is computed by;

$$C(\varepsilon) = \frac{2}{N(N-1)} \sum_{i=1}^{N} \sum_{j=i+1}^{N} H(\varepsilon - \|\mathbf{s}_i - \mathbf{s}_j\|) \tag{2.5}$$

where $\|\bullet\|$ represent vector distance (euclid distance of two vectors) and H is the heaviside step function.
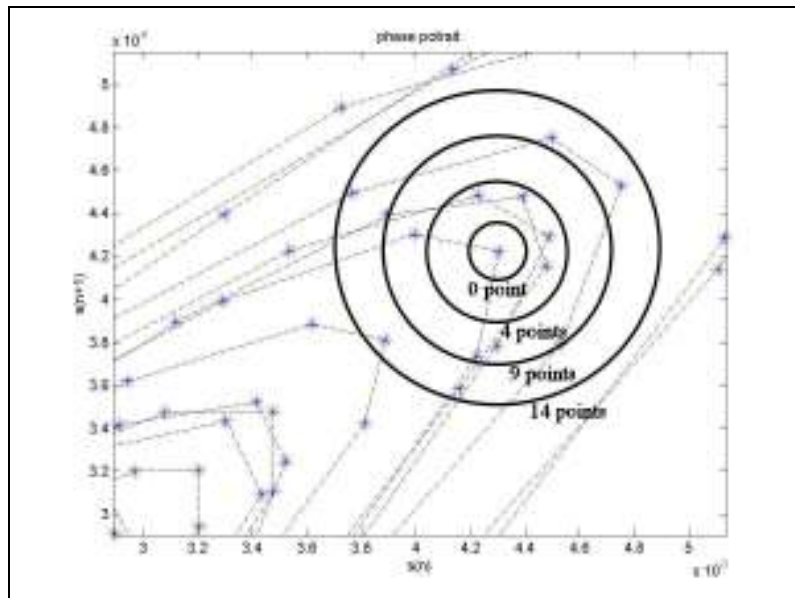
Figure 2.4. Correlation sum demonstration

However, in a typical time series, the samples have correlation with each other when they are close in time, besides of having correlation according to attractor geometry. This kind of temporal correlations are excluded from the correlation sum by updating the correlation sum formula;

$$C(\varepsilon) = \frac{2}{(N-n_{min})(N-(n_{min}-1))} \sum_{i=1}^{N} \sum_{j=i+n_{min}}^{N} H(\varepsilon - \|\mathbf{s}_i - \mathbf{s}_j\|) \tag{2.6}$$

Here, n_{min} values can be chosen generously as long as n_{min}<< N. The n_{min} value is not large enough if it's taken as the first zero of the autocorrelation or decay of autocorrelation, so a bigger value than that must be chosen.
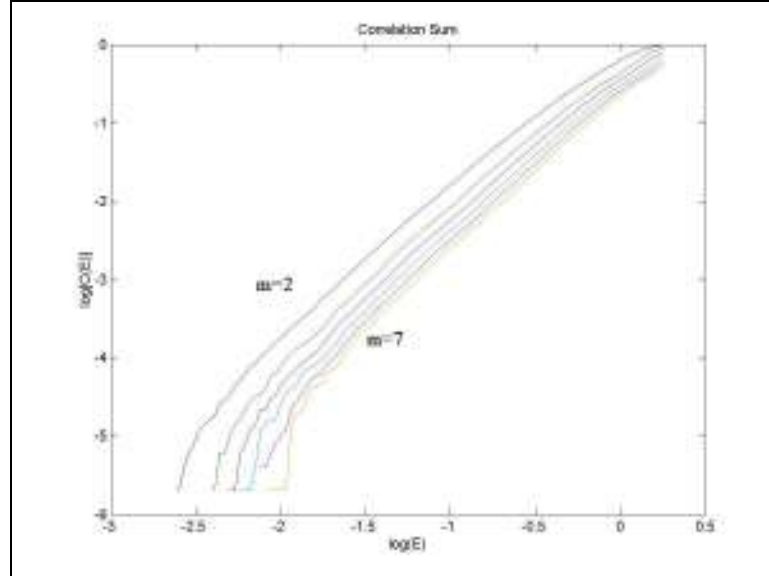
Figure 2.5. The correlation sum graph of Rössler system

The correlation sum just counts the pairs (**s**$_i$ **s**$_j$) whose distance is smaller than ε. In the limit of an infinite amount of data ($N \rightarrow \infty$) and for small ε, it is expected that C to scale like a power law;

$$C(\varepsilon) \ \alpha \ \varepsilon^{D} \qquad\qquad (2.7)$$

According to this power law property a dimension value $D,$ where based on the behavior of a correlation sum, can be defined as;

$$D(\varepsilon) = \lim_{\varepsilon \to 0} \lim_{N \to \infty} \frac{\log C(N, \varepsilon)}{\log \varepsilon} \qquad\qquad (2.8)$$

This dimension is called *correlation dimension* and it's a characteristic quantity for time series. Correlation dimension simply shows that how $C(\varepsilon)$ scales with ε. The local slopes of the correlation sum graph constructs correlation dimension graph, and the correlation dimension is equal to the average value of plateau region in the graph (Figure 2.6).
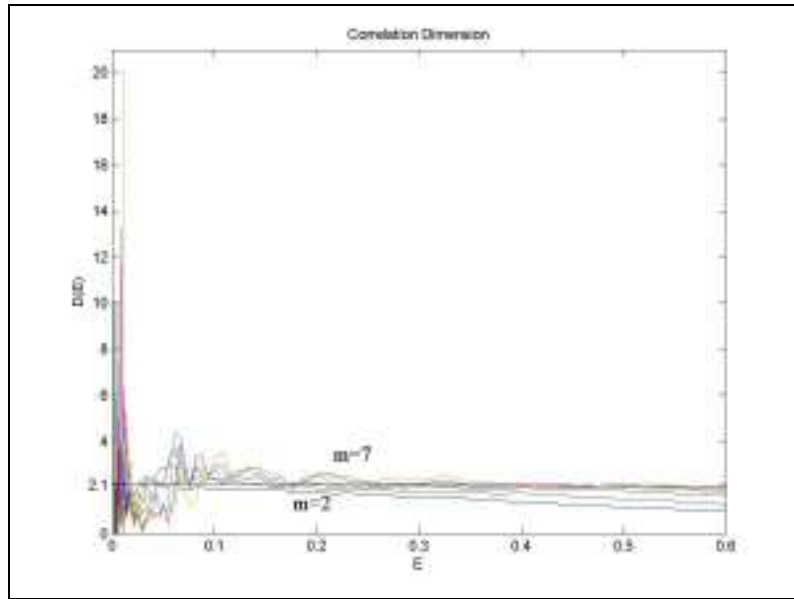
Figure 2.6. Correlation Dimension graph of Lorenz system

Correlation dimension can also be used to determine whether a time series derives from a random process or from a deterministic chaotic system. The variation of correlation dimension according to embedding dimension is used to characterize the time series in this mean. If the time series is a random process, $D(m)$ increases continuously. If the time series is a deterministic system, after some point D remains constant. A plot of the correlation dimension as a function of the embedding dimension indicates this property.

2.4.2. Lyapunov Exponents

The most important feature of chaos theory is the unpredictability of the long term future although it is a deterministic time evolution. In chaos theory, "similar causes have similar effects" belief is invalid except for short periods. Inherent instability of the solutions causes this unpredictability, which is called *sensitive dependence on initial conditions.*

Instability in time series leads two important concepts. Although they are related, they are mentioned as different concepts. These are; loss of information quantity as known as Kolmogorov – Sinai (metric) entropy, the other one is the simply exponentially separation of the nearby trajectories a.k.a. Lyapunov exponent (λ). Lyapunov exponent, which shows the long term behavior of the time series, is a

fundamental property that characterizes the rate of separation of infinitesimally close trajectories. Furthermore, the value of Lyapunov exponent represents the characterization of the system, e.g. if λ is positive, the nearby trajectories diverge exponential, which means existence of chaos.

Table 2.2. Characterization of the system via Lyapunov Exponents (Sprott 2003)

λ_1	λ_2	λ_3	λ_4	Attractor	Dimension
(-)	(-)	(-)	(-)	Equilibrium point	0
0	(-)	(-)	(-)	Limit Cycle	1
0	0	(-)	(-)	2-torus	2
0	0	0	(-)	3-torus	3
(+)	0	(-)	(-)	Strange (chaotic)	>2
(+)	(+)	0	(-)	Strange (hyperchaotic)	>3

Many different Lyapunov exponents can be defined for a dynamical system. It is a result of multi dimension of phase space. However the most important Lyapunov exponent is the one which is called maximal Lyapunov exponent.

Suppose that, in phase space, two points, which are close to each other with distance $\varepsilon_0 = \| s_{n_1} - s_{n_2} \|$, will diverge exponentially from each other after some step, and the distance between them becomes; $\varepsilon_{\Delta n} = \| s_{n_1+\Delta n} - s_{n_2+\Delta n} \|$. The relation with these two distances can be obtained by; $\varepsilon_{\Delta n} \cong \varepsilon_0 e^{\lambda \Delta n}$ where λ is the Lyapunov exponent of that trajectory. Moreover, for finding maximal Lyapunov exponent from reconstructed time series data, firstly average distinction is calculated as:

$$S(\Delta n) = \frac{1}{N} \sum_{n_0=1}^{N} \ln \left(\frac{1}{|U(\mathbf{s}_{n_0})|} \sum_{\mathbf{s}_n \in U(\mathbf{s}_{n_0})} \left| s_{n_0+\Delta n} - s_{n+\Delta n} \right| \right) \qquad (2.9)$$

where $U(\mathbf{s}_{n_0})$ is the neighborhood of $\mathbf{s}_{n_0}$ with diameter ε and s_{n_0} is the first element of $\mathbf{s}_{n_0}$. Then, if S exhibits a linear increase with identical slope, this slope can be taken as an estimate of maximal Lyapunov exponent (Figure 2.7).

In time series analysis, some modifications are applied to the data, e.g. rescaling, shifting, phase space reconstruction. Lyapunov exponents aren't affected by these modifications.

2.4.3. Metric Entropy (Kolmogorov – Sinai Entropy)

The metric (Kolmogorov – Sinai) entropy is a kind of measure to characterize chaotic motion of a system in an arbitrary-dimensional phase space. The metric entropy is proportional with the rate of loss of information at the current state of a dynamical system in the course of time. Meanwhile, metric entropy is a measure of the rate of lost of predictability, which indicates that how far into the future can be predicted with a given initial information. Metric entropy originate from information theory.

In time series analysis, information theory provides an important approach. If the observation of a system is considered as a source of information with a stream of numbers, then the information theory can supply quantitive answer to how much info can be possessed about the future when entire past have been observed. The metric entropy of a time series is;

$$K = \lim_{m \to \infty} \lim_{\varepsilon \to 0} \log \frac{C(m,\varepsilon)}{C(m+1,\varepsilon)} \qquad (2.10)$$

In metric entropy graph, estimated metric entropy is equal to the average value of plateau region in the graph (Figure 2.8).

Metric entropy has units of inverse time (for continuous systems) or inverse iteration (for discerete systems). The value of the metric entropy describes the type of system, e.g. in random systems, the metric entropy is equal to infinity (1/0, zero step ahead can be preticted), and in periodic systems, the metric entropy is equal to zero (1/∞, all the information can be preticted). Metric entropy can not take negative values and can be large for a chaotic system.
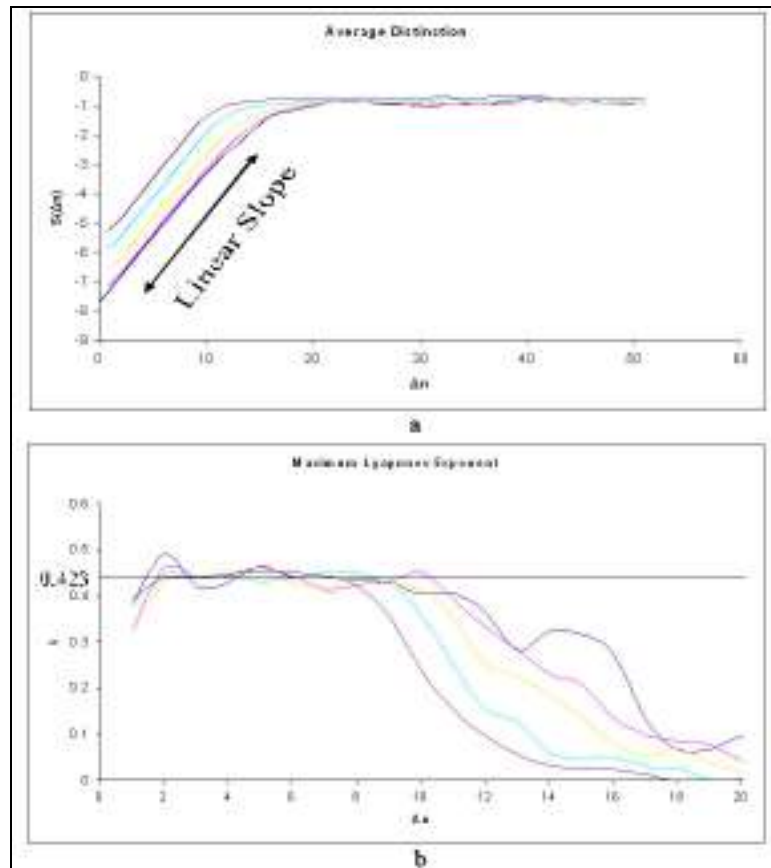
Figure 2.7. Estimation of maximal Lyapunov Exponent of Henon Map. In the graph (a),
average distinction is calculated for various ε values. (a) Average
Distinction (b) Maximum Lyapunov Exponent
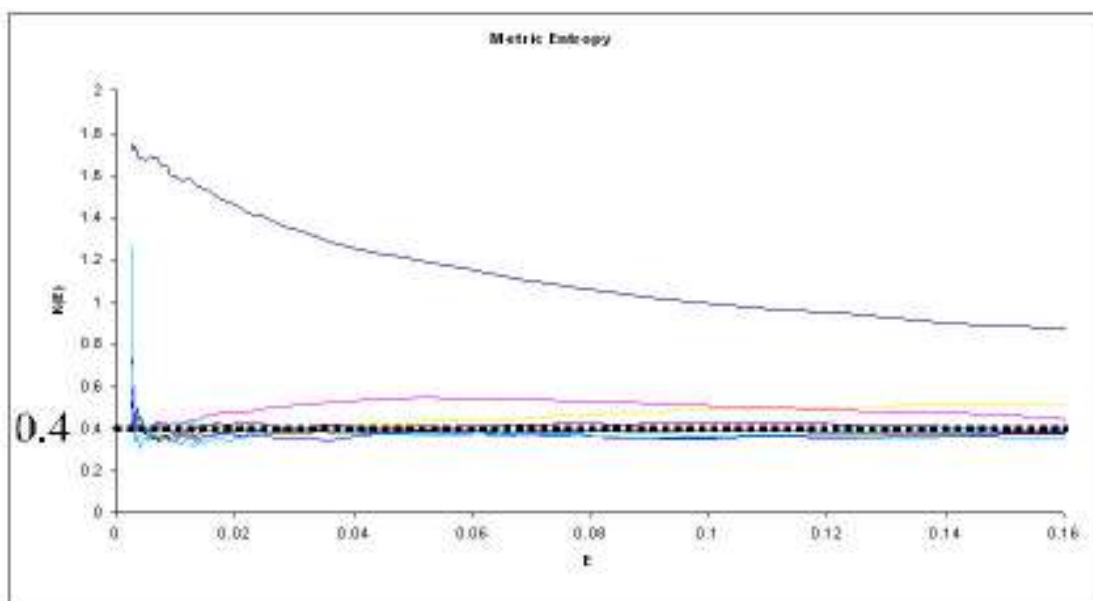
Figure 2.8. Metric Entropy of Henon Map which is calculated for embedding
dimensions 1 to 10

2.4.3.1. Pesin's Identity

Pesin's identity relates the sum of positive Lyapunov exponents to the entropy of the system. Lyapunov exponents, which measure the exponential rate of divergence of nearby trajectories, are related to metric entropy in a such way that the metric entropy is equal to the sum of the positive Lyapunov exponents only when the natural measure is continuous along the unstable directions, as it is usually the case for chaotic flows (Eq. 2.11). In 1977, Pesin proved that for certain classes of systems such as one dimensional maps, the logisitic map, henon map and tent map, the metric entropy is equal to the sum of positive Lyapunov exponents due to the fact that the system invariants are absolutely continues all expanding dimensions.

$$K = \sum_{i,\lambda_i>0} \lambda_i \qquad (2.11)$$

CHAPTER 3

IMPLEMENTATION OF NONLINEAR DYNAMICS
IN TIME SERIES

Beyond theoretical aspects, there are few concepts to be considered before the analysis of the time series. Computation of invariants should be performed after some tests and processes are applied to the experimental data. Also, some calculations of invariants need parameters which are optimized to constant values. For a proper usage of time series, preliminarily processes should be taken into consideration.

3.1. Stationarity

Stationarity is a property in which the mean, variance and autocorrelation structure remains constant over time, in other words, the distribution of the variables does not depend on time.

A first step in time series analysis requires to achieve stationarity in the data, thus the stationarity test has to be made. Stationarity test can be done in few steps, these steps are:

- Divide the series into equal length segments.
- Compute the mean value for each consecutive segment.
- Compare the segments' means with the mean of the whole series. Compute the standard error:

$$\sqrt{\frac{\sum_{n=1}^{N}(s-\langle s\rangle)^2}{N(N-1)}} \quad \text{where} \quad \langle s\rangle = \sum_{n=1}^{N} s_n / N \qquad (3.1)$$

In time series analysis, stationarity is quite important to satisfy that the invariants give the reliable results, while the series have no increasing or decreasing

trend, constant variance over time and constant autocorrelation structure. For instance, wherever the segment is taken from, the dynamics should remain the same.

3.2. Testing Nonlinearity

The nonlinear analysis of time series use techniques for the underlying nonlinearity which exists in time series. Indeed, the stochastic linear systems may have very complicated structure. Even so, the application of nonlinear series methods has to be guaranteed by determining the nonlinearity in the time series which will be analyzed. Hence, before starting to analyze a time series by nonlinear techniques, it is needed to apply nonlinearity test to the data. In this study, nonlinearity test is achieved by the method of surrogate data.

3.2.1. Method of Surrogate Data

Surrogate data is way of describing time series, whether it derives from nonlinear deterministic system or some linear process. For this purpose the *null hypothesis* which consists of candidate linear process is created. The objective is to reject the hypothesis. A typical null hypothesis would be that the data result from Gaussian linear stochastic process.

3.2.1.1. Null Hypothesis (ARMA)

Autoregressive (AR) models include past observations of the dependent variable in the forecast of future observations and moving average (MA) models include past observations of the innovations noise process in the forecast of future observations of the dependent variable of interest. Autoregressive-moving-average (ARMA) models are time-series models that include both AR and MA components. Shortly, ARMA indicates linear models of the autocorrelation in a time series. ARMA models can be described by a series of equations.

$$s_n = a_0 + \sum_{i=1}^{M_{AR}} a_i s_{n-i} + \sum_{j=0}^{M_{MA}} b_j \eta_{n-j} \tag{3.2}$$

Here η is independent Gaussian random numbers with zero mean and unit variance and M_{AR} and M_{MA} are the orders of the ARMA process respectively, e.g. if the order of autoregressive part is one $M_{AR} = 1$, and the order of the moving average part is two $M_{MA} = 2$, then the ARMA process is expressed as ARMA (1, 2).

After creating surrogates, a statistics must be chosen to make comparison. This statistics can be linear or nonlinear prediction error, two or more point correlation, any kind of dimension etc. The task is to calculate this statistics for null hypothesis, data and its surrogates, then to make comparison between the results. The deviation of results of original data and its surrogates from result of null hypothesis, point out that the original data doesn't come from a linear process. Some of the statistics for making comparison between null hypothesis and original data with its surrogates are shown below;

- **Linear Prediction Error**

Linear prediction and linear prediction error calculations are shown below;

$$\hat{s}_{n+1} = a_0 + \sum_{i=1}^{M_{AR}} a_i \hat{s}_{n-M_{AR}+i} \tag{3.3}$$

where $\hat{s}$ shows the predicted value. The coefficient a_0 can be omitted by subtracting the mean from the data; $\bar{s}_n = s_n - \mu$. The coefficients a_i are determined by a best fit to whole time series.

$$\sum_{i=1}^{M_{AR}} c_{iq} a_i = \sum_{n=M_{AR}}^{N-1} s_{n+1} s_{n-M_{AR}+q} \tag{3.4}$$

where c_{iq} is the autocovariance matrix and $q=1$ to M_{AR}

$$c_{iq} = \sum_{n=M_{AR}}^{N-1} s_{n-M_{AR}+i} s_{n-M_{AR}+q} \tag{3.5}$$

The illustration of computing coefficient a_i is shown below;

$$\text{For} \quad M_{AR} = 1 \; ; \qquad a_1 = \frac{\sum\limits_{n=1}^{N-1} s_{n+1} s_n}{\sum\limits_{n=1}^{N} s_n^2} \qquad (3.6)$$

$$\text{For} \quad M_{AR} = 2 \; ; \qquad a_1 = \frac{\sum s_n s_{n-1} \sum s_{n+1} s_n - \sum s_n^2 \sum s_{n+1} s_{n-1}}{\left(\sum s_n s_{n-1}\right)^2 - \sum s_n^2 \sum s_{n-1}^2} \qquad (3.7)$$

the sums are

from $n = 2$ to N

$$a_2 = \frac{\sum s_n s_{n-1} \sum s_{n+1} s_{n-1} - \sum s_{n-1}^2 \sum s_{n+1} s_n}{\left(\sum s_n s_{n-1}\right)^2 - \sum s_n^2 \sum s_{n-1}^2} \qquad (3.8)$$

After creating the linear predictions of time series, the prediction error e is computed for data sets. Root mean square (rms) prediction error is;

$$e = \sqrt{\left\langle \left(\hat{s}_n - s_n\right)^2 \right\rangle} \qquad (3.9)$$

- **High order correlations**

Higher order correlation calculations can be used because they are fast in computational time. Although the correlations are based on linear relations, higher-order autocorrelation measures the time asymmetry which is a strong signature of nonlinearity. One typical q^{th} order quantity is;

$$\frac{1}{N-v} \sum_{n=v+1}^{N} (s_n - s_{n-v})^q \qquad (3.10)$$

The goal is making a comparison between null hypothesis and original data with its surrogates, according to the results of the statistics chosen. For this purpose, surrogates are created (Figure 3.1). Surrogate data sets should satisfy that they contain correlated random numbers which have the same power spectrum as the original data. The number of surrogates is computed by specified *level of significance.* For significance of 95%, 19 surrogates must be created for testing (19 surrogates and one original data make a total number of 20 time series. 1 in 20, 5%). For the purpose of creating surrogate data, first of all, fast (discrete) Fourier transform of data is taken;

$$\ddot{s}_k = \frac{1}{\sqrt{N}} \sum_{n=1}^{N} s_n e^{i 2\pi k n / N} \tag{3.11}$$

where k is between zero and N. Then $\ddot{s}_k$ values ate multiplied by random phases, $\widetilde{s}'_k = \ddot{s}_k e^{i\phi_k}$ where ϕ_k are uniformly distributed in $[0,2\pi)$. Finally, inverse FFT is computed.

$$s'_n = \frac{1}{\sqrt{N}} \sum_{k=1}^{N} \widetilde{s}'_k e^{-i 2\pi k n / N} \tag{3.12}$$

After creating the surrogates, the statistics all K surrogate data sets are computed. If the major statistic results of original and surrogate data sets deviate from null hypothesis result, then the null hypothesis can be rejected. That majority is determined by significance level (e.g. 19 of 20 data sets in 95% significance level). Rejection of null hypothesis indicates nonlinearity of the time series. Otherwise, the series are based on a linear process.
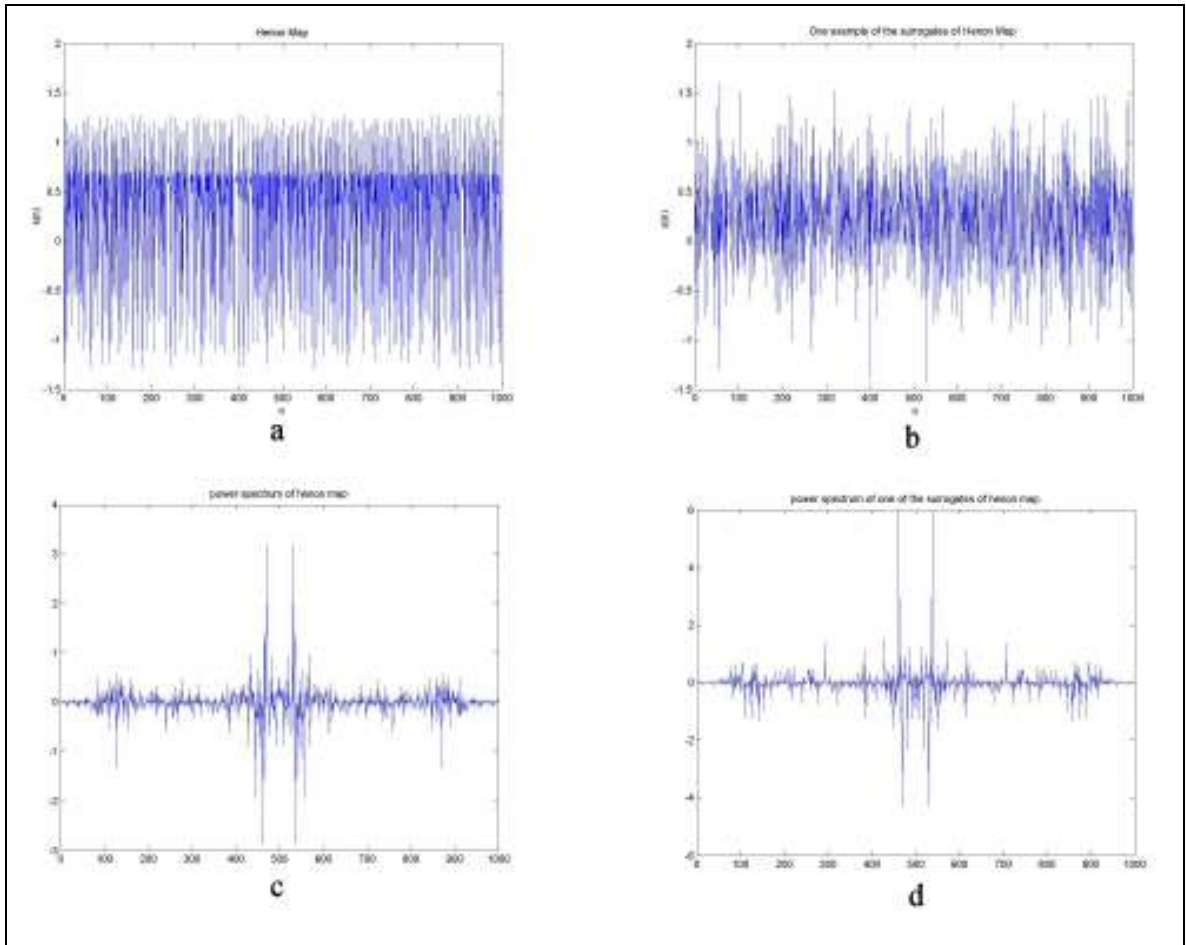
Figure 3.1. Surrogate data of Henon map. (a) Original time series of Henon map
(b) One of the examples of the surrogates of Henon map (c) Power spectrum
of original series of Henon map (d) Power spectrum of one of the examples
of the surrogates of Henon map

3.2.2. Visual Inspection

Alternatively, testing nonlinearity process can be performed by using visual inspection from embedding dimension- correlation dimension graph. In chaotic time series, correlation dimension of a time series levels off at certain point in embedding dimension- correlation dimension graph. However, the surrogate data of that series continue increasing in correlation dimension monotonically with increasing embedding dimension.

The major purpose can be achieved by demonstrating embedding dimension-correlation dimension plot of original data and its surrogate. The convergence of

26

original data and continues increment of its surrogate are sufficient to indicate that the original data might not come from a linear stochastic process (Figure 3.2).
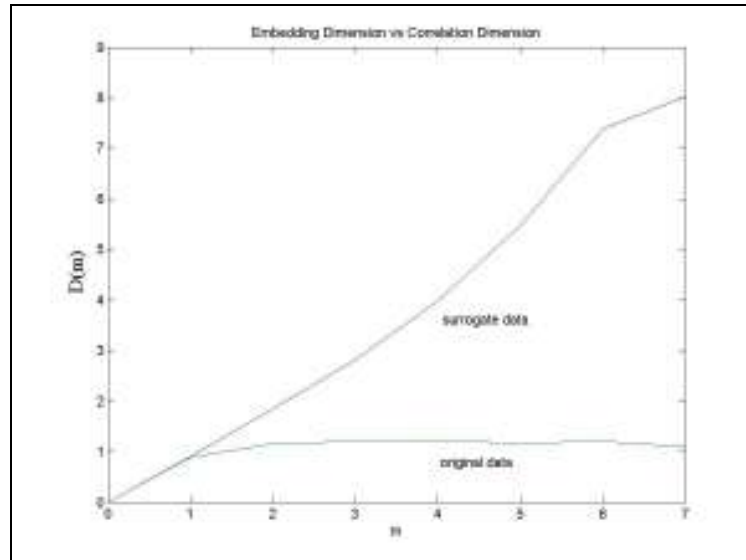

Figure 3.2. Testing nonlinearity by using visual inspection from embedding dimension-correlation dimension graph.

3.3. Nonlinear Noise Reduction (State – Space Averaging)

A time series with noise can be described in two components; one contains the signal, and the other one contains random fluctuations. The classical way to identify these two components is applying time series to power spectrum to obtaining the distinction and then using a filter for separation (e.g. Wiener filter). However, this approach fails for deterministic chaotic time series. The reason of failure comes from property of that kind of system. Such systems produce a broad band spectrum in which power spectrum of the signal resembles the power spectrum of random noise.

Alternatively, a better approach, which is called nonlinear noise reduction (a.k.a. state space averaging), can be used (Figure 3.3). Nonlinear noise reduction is process which noisy measurements are replaced by better values. The process simply follows few steps shown below;

- Reconstructing the embedding phase space,
- Finding the vectors $\mathbf{s}_n$ which are in the ε neighborhood of $\mathbf{s}_{n_0}$, $\left\| \mathbf{s}_{n_0} - \mathbf{s}_n \right\| < \varepsilon$,
- Taking average of middle values (at $[m/2]^{th}$ column) of these vector,
- Replacing the original values with the new, averaged values ($\widehat{s}$);

$$\widehat{s}_{n-(m/2)} = \frac{1}{\left| U(\mathbf{s}_{n_0}) \right|} \sum_{\mathbf{s}_n \in U(\mathbf{s}_{n_0})} s_{n-(m/2)} \qquad (3.13)$$
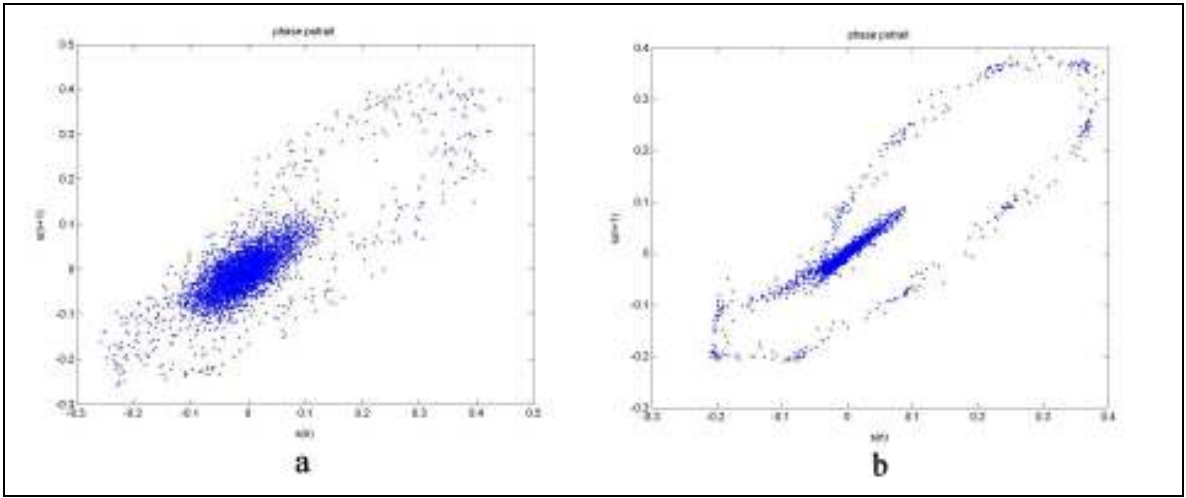

Figure 3.3. Phase Portrait of ECG data (a) Before noise reduction (b) After noise reduction

In this algorithm, embedding dimension m should be taken a value that is higher than m value needed by embedding theorems. Also, the neighborhood value ε should be taken a value that is large enough to cover the noise size. However, ε value should also be smaller than a typical curvature radius which exists in the time series. In this approach, for the first and the last $m/2$ values of the time series, there is no correction available. This algorithm allows applying multiply iterations with decreasing ε values until no further change can be observed.

3.4. Tsonis Criteria

In time series analysis, the representation of the attractor is bounded with the number of data. In order to make a confidential analysis of time series, complete representation of the attractor and its geometric behavior should be satisfied. For a finite

data set, as the attractor dimension gets bigger, more data points are required to determine its dimension. At this point, the term of required number of data points is counted to the consideration. In the literature, controversial approximations exist. However, the compromise suggestion about the required data points came from Tsonis (1992). From his definition, the minimum sufficient data points for time series analysis is obtained by;

$$N_{\min} \alpha \, 10^{2+0.4D_A} \tag{3.14}$$

where D_A is the attractor dimension. Additionally, from this equation, the highest embedding dimension can be obtained from given N data point;

$$D_A \alpha \, 2.5\left[\log(N) - 2\right] \tag{3.15}$$

Even though there is no guarantee for sufficiency of calculation the data points from this equation, plausible estimations of necessary data can be achieved.

3.5. Finding Optimum Embedding Dimension

Finding optimum embedding is a significant process while it determines the optimum reconstructed dimension which can be satisfactory for complete representation of actual phase space. Due to the fact that deficient embedding dimension has not the same geometric properties as the attractor in actual phase, the analyses, the computation of the invariants and the conclusion results would be incorrect. Although, in this study, constant embedding dimension value is not used for some invariants' computation, such as correlation dimension, calculation of all Lyapunov exponents of the system requires a constant optimum embedding dimension.

3.5.1. False Nearest Neighbor

Suppose that, for a given time series, required minimal embedding dimension is m_0. This means that the time series should be reconstructed at least in m_0, on the condition that the reconstructed attractor is a one-to-one image of the attractor in the

original phase space. If time series is reconstructed to an smaller embedding dimension than minimal embedding dimension, then the state space trajectories projection of the points might appear as near neighborhoods of other points which they are not neighbor in actual. These points are called *false nearest neighbors.*

To pass over this problem, it would be useful to increase the embedding dimension step by step beginning from small values while controlling the false nearest neighbors in each embedding. As the embedding dimension increases, the false nearest neighbors to a particular point in the embedding space should decrease until the embedding dimension is sufficiently large to cover the geometry of the attractor in phase space. This algorithm is called the false nearest neighbor method which is a method to determine the minimal sufficient embedding dimension introduced by Kennel et al. in 1992 (Figure 3.4). The idea of this algorithm is the following:

- Find the nearest neighbor of each point in *m*-dimensional space,
- Calculate the distance,
- Iterate both points, calculate the distance and compute the ratio:

$$R_i = \frac{\left\| \mathbf{s}_{i+1} + \mathbf{s}_{j+1} \right\|}{\left\| \mathbf{s}_i + \mathbf{s}_j \right\|} \tag{3.16}$$

The criterion for selection of the required minimum embedding dimension is that the ratio of different embeddings converges at some point. The designation of the false nearest neighbors is essential for the calculation of invariants, like the correlation dimension, especially the Lyapunov exponent.
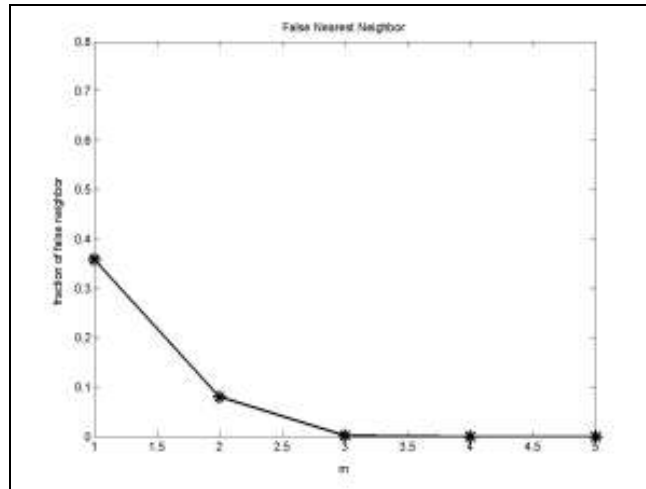
Figure 3.4. False nearest neighbor graph of drill vibration data

3.5.2. Embedding Dimension – Correlation Dimension

Another method for obtaining optimum embedding dimension is the visual inspection from embedding dimension – correlation dimension graph. It is a fact that in chaotic time series, correlation dimension for increasing embedding dimension become constant after a saturation dimension level. In this way, optimum embedding dimension can be found as computing correlation dimension for various embedding dimensions and plot the results. In that plot, the level of embedding dimension where the correlation dimension converges is accepted as the optimum embedding dimension (Figure 3.5).

3.6. Practical Considerations of Processing Time Series

In time series processing, an important concept, sampling rate, must be considered to fulfill the desired data acquisition.

3.6.1. Nyquist Sampling Rate Theorem

Sampling is a process which consists of converting a continuous time signal into a discrete time sequences. Discrete samples are a complete representation of the signal, hence sampling rate, which is the interval of it discrete moments of time, is very significant, because it would obtain how much detail the samples have about the signal.

According to the *Nyquist Sampling Theorem*, for the purpose of having no loss information about the signal, the sampling rate should be greater than or equal to twice the highest frequency present in the signal. When a signal is not sampled at a high enough rate, aliasing occurs.

3.6.1.1. Aliasing

In sampling, the sampling rate should be at least twice value of the highest frequency which exists in the signal. If the sampling rate is not high enough to sample the signal correctly then a phenomenon called *aliasing* occurs. Mainly the term aliasing refers to incorrect representation of the actual signal by the distortion which has a base from lack of sampling rate. Moreover, aliasing indicates that the components of the signal at high frequencies are replaced with components at lower frequencies by mistaken.
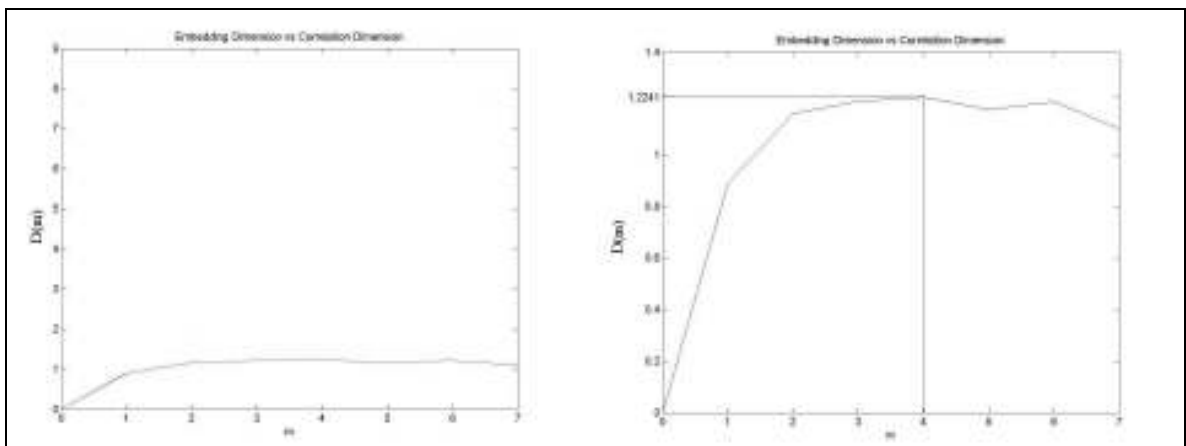

Figure 3.5. Embedding Dimension vs Correlation Dimension graph of Henon map

3.6.2. Time Series from Vibration Signal

In recent years, the most commonly used method for condition monitoring of rotating machines is the vibration measurement and analysis, because, the parameter which can be measured without stopping an equipment and which will give the maximum information about its working condition is vibration. The vibration of a machine is response of that machine to the forces caused by moving parts. However, it

is not the only cause of machine vibration. Suppose that a machine force is producing a frequency of *f* and this force does not contain any other frequency. Because of the nonlinearity of mechanical structure of the machine, this *f* force will extend in magnitude, and can cause the vibration will occur at harmonics of *f* as well as *f*. Moreover, the connected materials, e.g. tool ends, can cause nonlinearity when they are misaligned. Besides this, their vibration signature contains a strong second harmonic of *f*. Also consecutive connections which are misaligned can often produce a third harmonic of *f*. The outcome of forces acting at different frequencies, show itself by the generation new frequencies that do not exist in the forcing functions themselves. The new frequencies, which are the sum and difference frequencies, cause breakage of tool bit, defection of gearboxes, rolling bearings, etc. Moreover, one the reasons of generation of new frequencies which are not exist in the forcing functions is the modulation.

Vibration analysis as a condition monitoring system consists of measuring sequence of data points at equal time intervals from the machine via sensors and performing the computations invariants by means of applied monitoring technique. Consecutive data measurements form time series which are commonly measured by accelerometers.

3.6.2.1. Accelerometer

An accelerometer is a device for measuring acceleration, shock or vibration. Accelerometers are used as in many other scientific and engineering systems such as condition monitoring, automotive, medical, etc. One of the most common uses for accelerometers is in airbag deployment systems for modern automobiles. When a collision or impact has occurred, the accelerometers detect the severity of it by the rapid deceleration of the vehicle.

The most commonly used type of accelerometers is the piezoelectric accelerometer in which sensing element is a crystal which has the ability of emitting a voltage when subjected to a mechanical stress. This crystal is bonded to a mass such that when the accelerometer is subjected to a 'g' force, the mass compresses the crystal. In this manner, the crystal emits a signal which is related to the imposed 'g' force.

The location of the sensor is another significant feature. The vibration can be measured at various locations on the machine to infer the magnitude of the forces from these vibrations. However, it is very important that placing the sensor as closer as possible to the component which is desired to be monitored.

CHAPTER 4

METRIC ENTROPY APPLICATIONS
FOR CONDITION MONITORING

Condition Monitoring is the process which represents the use of advanced technologies to determine equipment condition, and potentially indicate the development of probable failure in machinery. Condition Monitoring is a major component of the predictive or condition-based maintenance techniques. Even so, with condition monitoring, avoidable actions can be performed before the failure occurs, or the schedule of the maintenance can be achieved. Condition monitoring is much more cost effective while it can prevent the machinery component from failing. Condition monitoring is widely used in rotating machineries.

4.1. Experimental Setup

The aim of this study is to check the availability of creating a diagnostic and prognostic mechanical condition monitoring system, by the means of nonlinear dynamics. That is an introduction to a system which is equipped with intelligent fault detection. Time series implementations on bearings and drill bits are performed. For the ball bearing failure experiments, two different test rigs were created, but none of them was successfully completed. Therefore, a third test rig for the drill bit breakage was constructed.

4.1.1. Ball Bearing Failure Test Rig I

Most bearing fault detection application deals with pre-defected ball bearings where the bearings exhibit mature faults. Damages were seeded to the bearing typically by drilling the surface, or machining with an electrical discharge. Although, run-to-failure experiments were planned in this study, small dents were created on the ball surface of the bearings.

The schematic of the bearing test rig is shown in Figure 4.1. The rig contains a shaft which was connected to the motor with a coupling arrangement. The shaft was supported by two bearings at its ends. The coupling ensures that the shaft is not effected from any of the vibrations from the motor, accommodating any misalignments present in the assembly.
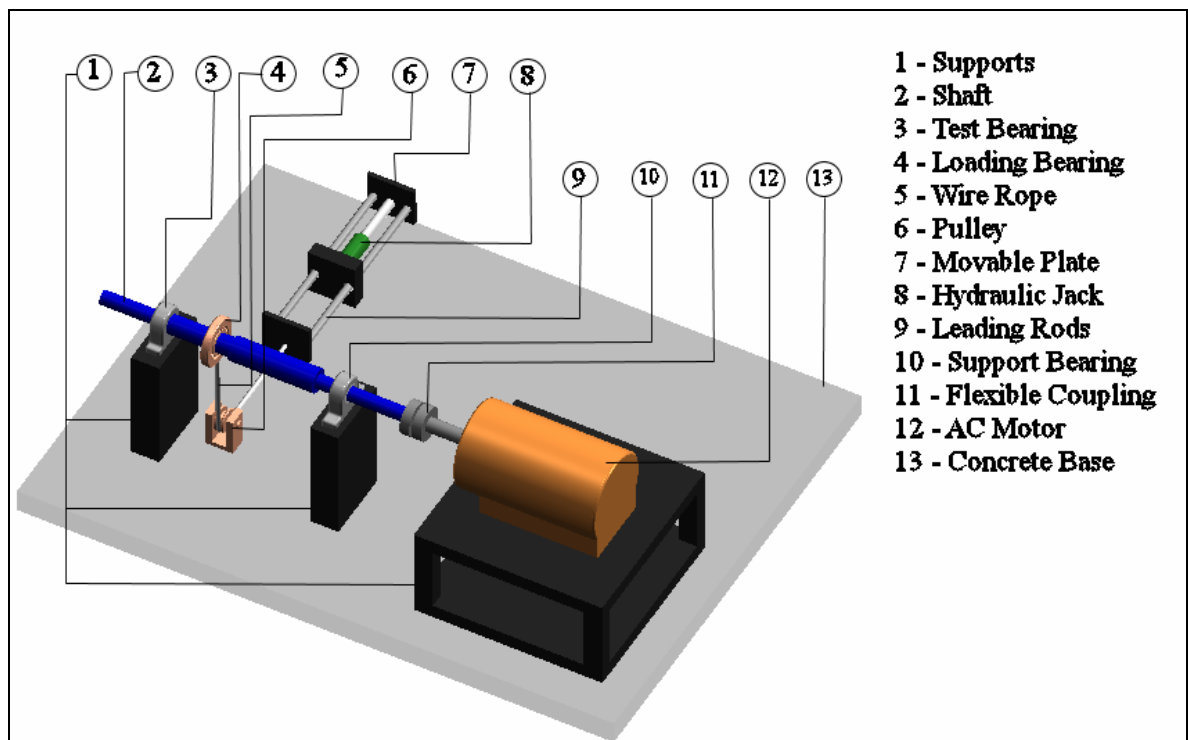

Figure 4.1. Schematic of bearing test rig I

In the test rig, AC motor which has maximum 3000 rpm rotation speed was used. The support bearing and the test bearings were selected as UBC UC206 single row deep groove ball. The loading of the shaft is done through an UBC UC210 heavy duty deep groove ball bearing. This load bearing is mounted in between the test bearing and the support bearing, where it was kept near to the test bearing, as a purpose of the fact that major of the load was transferred to the test bearing. Therefore, by this configuration three-quarters of the load applied was acting on the test bearing. The load bearing, which is equipped with the housing, was pulled by a wire rope and pulley arrangement.

The hydraulic jack with a pressure gauge was operated with a manual hydraulic pump. A piezoelectric accelerometer was placed on the housing of the test bearing.

Detailed information of the accelerometer and data acquisition can be found in section 4.1.3 and on Table 4.1.

Before the experiment, dents on the bearing's ball were created by using EDM (electrical discharge machine) in order to keep size and depth of the dent under control (Figure 4.2). Dents were seeded in three different sizes, one was about 1 mm in diameter and 1 mm in depth, the other one was 2 mm in diameter and 1 mm in depth, and the last one was 2 mm in diameter and 2 mm in depth.

Figure 4.2. The dents on the surface of the ball of bearing

After allowing the bearing to initial run for while, vibration data was collected at a sampling rate of 192 KHz for 0.1 seconds long. The hydraulic jack was adjusted at 42 bars that equals to acting 5kN force on loading, 3.8kN force on test bearing (Figure 4.3).

Figure 4.3. (a) The experiment rig for ball bearing testing (b) Adjusted value of the
hydraulic jack shown in barometer

Although all the force and torque calculations were computed with great margin
to avoiding failure of a component other than test bearing, after 6 hours run time, the
shaft of the motor was broken down. According to that failure, experiments on test rig I
were canceled. Substitute to test rig I, a new, small scaled bearing test rig was designed.

4.1.2. Ball Bearing Failure Test Rig II

A small scale of test rig I was built(Figure 4.4). The bearing test rig II consists
of one shaft, an ac motor, 2 supporting and as a test bearing one load bearing. After the
experiences which were gained from the previous test rig, two bearings were selected as
supporter, and the test bearing became the loading bearing itself. Also, in test rig II, no
primary fault was created on the test bearings. Because of the lever type loading, a
weight of 30 kg on the end of the force arm created a 2kN force on the test bearing.
Similarly in the test rig I, after allowing initial running, vibration data was collected at a
sampling rate of 192 KHz for 0.1 seconds long via accelerometer. But again, after 1
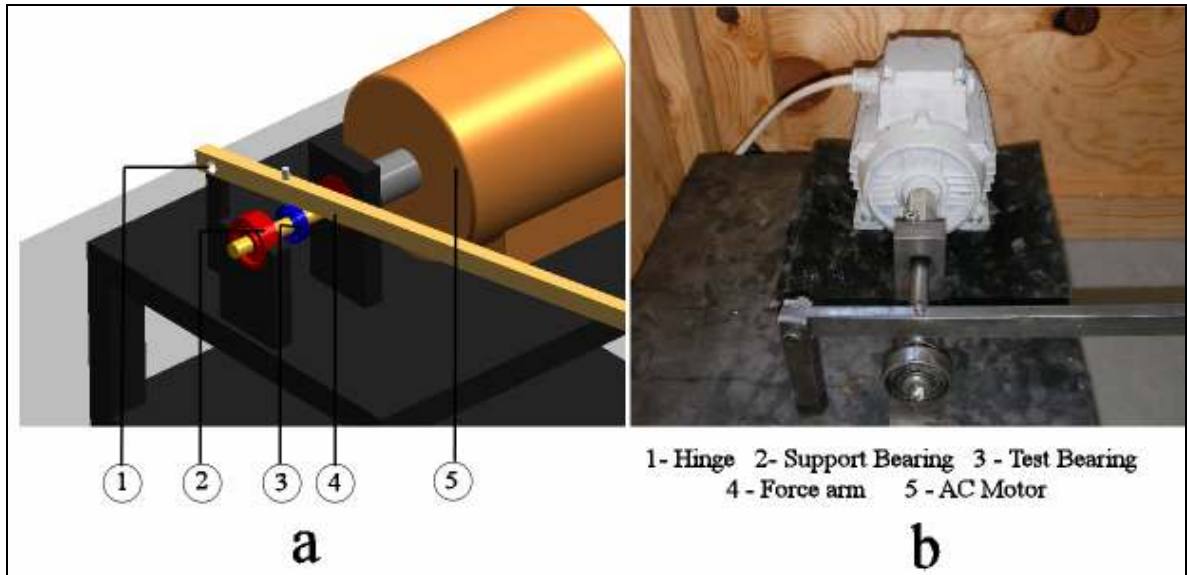day, the shaft of the system failed.

Figure 4.4. (a) Schematic of test rig II (b) A view of bearing test rig II

According the failures which happened during the tests, run-to-failure experiments on ball bearings were held. Replacing the experiments, machine tool breakage test were decided to be performed. For this aim, small drill bit breakage test rig was constructed.

4.1.3. Drill Bit Breakage Test Rig

The experimental setup for prediction of small drill bit breakage is shown in Figure 4.5. The test rig comprises PCB (printed circuit board) drill, drill stand, drill bit, scale weight, accelerometer, power supply/coupler and a personal computer.

The 4 Channel Piezoelectric Sensor Power Supply/Coupler (Kistler 5134A1E) provides constant current excitation required by accelerometers and decouples the DC bias voltage from the output signal. Ceramic Shear triaxial accelerometer (Kistler 8762A50) measures vibration simultaneously in three axis with high sensitivity. Computer based oscilloscope (Virtins Sound Card Oscilloscope) is used for online observation of vibration signal. Virtins software allows digitizing and acquiring the vibration data into a personal computer for further processing and analysis.
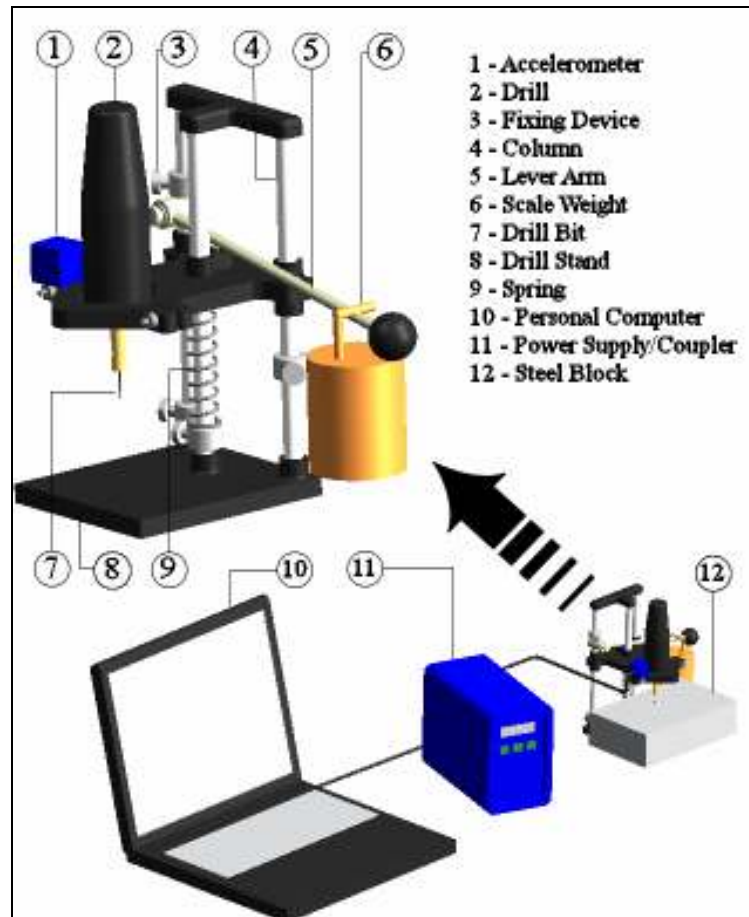
Figure 4.5. The schema of the test rig for drill bit breakage

Drill stand with lever-operated drill feed mechanism was used in experiment setup. Drill stand has a sturdy column base with springs for smooth plunge action, and also it has an adjustable depth stop and depth fixing device for controlled and measured cuts, while an ECB drill, which has a 12-18 volt DC motor with maximum output 22000 rpm, was fixed on it. Small high-speed steel (HSS) twist drill bits (1mm) were used during the experiments. As a drilling material, high carbon steel block is used because of its great hardness and brittleness which ensure that the drill bit is subjected to more torque and thrust force.

Table 4.1. Specification of experiment setup components

Drill		Drill Stand	
12-18 V DC motor	Approximate 1A	Total Height	210 mm
Output Power	16-40 Watt	Base Dimension	100x200 mm
Total rpm	15-22 000 rpm	Drilling Depth	30 mm max.
Squeezing capacity	0.5-3 mm	Height Adjustment	0-100 mm

Power Supply/Coupler		Accelerometer	
Frequency Range (with 30 kHz Filter)	0.036......30 kHz	Frequency Response ($\pm\%5$)	0.5....6000 Hz
Lowpass Filters (cut-off frequencies)	100, 1k, 10k, 30 kHz	Sensing Element	Ceramic/Shear
Output Voltage	± 10 V	Output Voltage	± 5 V
Output Current	± 5 mA	Source Constant Current	2.....18 mA

4.2. Data Analysis

Drill bit breakage tests were performed by drilling the steel block with 1mm drill bits. Drill bits were mounted to the drill, while the drill was fixed to the drill stand with same height and plunge depth arrangement repetitively. Meanwhile for the feeding process, scale weight was hung to the end of the lever arm to provide a constant feed rate for the drill. After the adjustment of the experimental setup, drilling started until the drill bit breakage was observed. At the same time, vibration signals were taken by the accelerometer in constant time intervals while the drilling process was continuously running. The signals were firstly passed though coupler which was set with low-pass filter (cut-off frequency: 30 kHz), and the signals were sent to a computer. Analog signals were converted to digital data by sound card of the computer, and the vibration data was stored using Virtins software with 192 KHz sampling rate. The sampling rate and cut-off frequencies were set to maximum values which the present experiment equipments allow. Furthermore, high sampling rate provides confidence to avoid aliasing.

A successful tool breakage prediction method must be sensitive to tool change in tool condition, but insensitive to the variations of drilling conditions. Therefore, drilling tests were performed at different conditions to evaluate the reliability of the experiment. However, only one orientation of drill speed, drill bit diameter, scale weight, lever position and mount length gave results successfully consistent.

Generally, drill bit breakage, which is caused by buckling and fluctuations in the cutting force, is a major problem with small drill bits of 2 mm or less. Indeed, the amount of feed, as well as the torque and thrust force, become too big for its diameter, and tend to cause breakage in small drill bits. On the other hand, with drill bit of standard size of about 3 mm or more, drill bit breakage is not a major problem, because as the diameter increases, the drill bit becomes rigid and tends to wear out instead of breaking. Therefore, 1mm diameter drill bits were used for testing. For instance, 1.5 mm and 2 mm diameter drill bits were also tested but no drill bit breakage was observed at all.

Different drill speeds were also tested. The drill, which was used in experiments, has 12-18 volt DC motor. The maximum output power is 40 watt with 22000 rpm. However, the drill speed adjustment is restricted with another variable; temperature. While 15 and 18 volt drilling attempts, very high temperature rise was observed which can damage the drill motor. Hence, the drill speed was set to 15000 rpm with 12 volt.

Eventually, the different lever height and scale weight adjustments were tested. 20, 50, 100, 200 and 500 grams of scale weights were located individually to the end of the lever arm. In each scale weight, different lever positions were also tested. Unfortunately in all that orientations rapid breakage or no breakage was observed. None of the adjustments gave a consistent result except one, 500 grams scale weight. With 500 grams scale weight, from the moment equation, it is calculated that approximately 20N force is applied to the drill downwards as feeding (Figure 4.6). So that, with this experiment adjustment, 1 mm drill bits can have a consistent 5-10 minute drill bit life. The small variation of the drill life is based on the drill bits production processes.

The vibration data of the setup was taken in every minute until the bit was broken down. All the measurements were 0.1 seconds long which equals to 19200 samples in each measurement. This sample number allows correctly representing the systems which have attractor dimension equals to 6, according to Nquist Sampling Rate Theorem. Although much more drill bits broke down, data acquisition of 10 drill bits successfully accomplished (Figure 4.7).
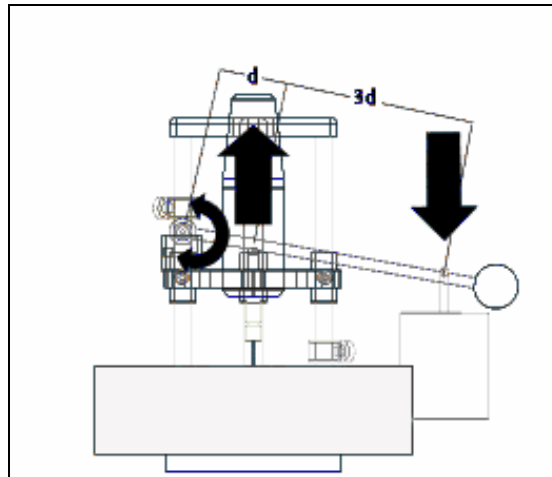
Figure 4.6. Schematic of lever force diagram

Figure 4.7. The broken drill bits

4.3. Experimental Results

The time series of the drill bit breakage prediction experiment were firstly tested for nonlinearity with surrogate data method (Figure 4.8). The visual inspection of distinction in embedding dimension – correlation dimension graph between original data and surrogate data was used to determine the nonlinearity. Moreover, nonlinear noise reduction process was applied to the series. However, because of the noise reduction algorithm's method as state averaging, some parts of original signals were lost

during the process, thus the dynamical behaviors could change as a results of this algorithm. Therefore, original noisy data was used for the analysis.
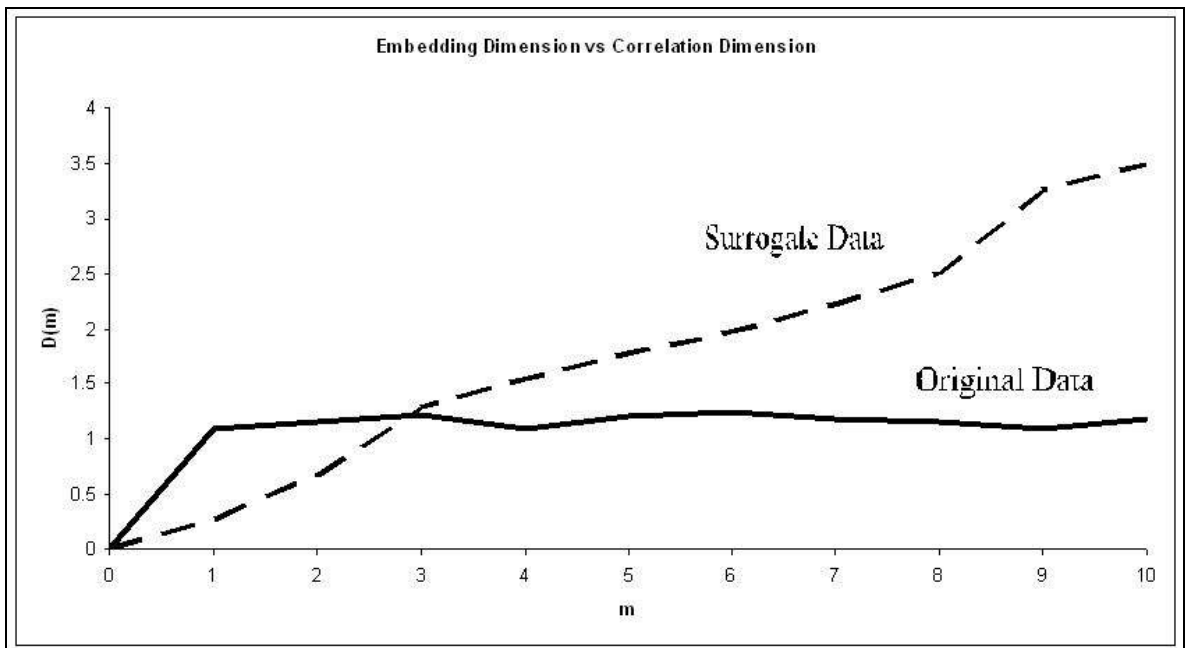
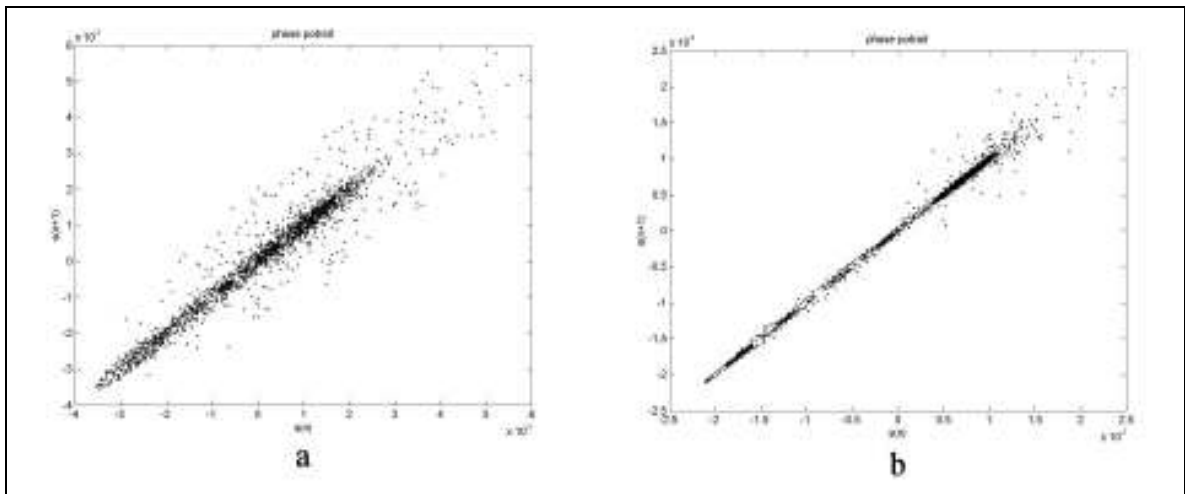Figure 4.8. Nonlinearity test of drill bit 3 with surrogate data

Figure 4.9. Noise Reduction Process of drill bit 5 (a) Before Noise Reduction (b) After Noise Reduction

Not only the chaotic variants were computed for the series, the time series statistical parameters were also taken in to account. RMS, kurtosis, skewness, crest factor values of all the series were calculated. Finally, the chaotic variants of series were obtained.

After the long computation period, database of drill bit breakage experiment was achieved. On a global models, backpropagation ANN, system modeling was attempted, but not be accomplished, due to the fact that drill bits with the same remaining life have not the same range for the all calculated values. Therefore, the suitable similarities in variation of the values were sought. But again, no consistent relation occurred, except for the metric entropy. Only the metric entropy variation of the drills during the life time seemed consistent (Figure 4.10, and 4.11). In 7 of 10 drill bits' variation of metric entropy, just one time step before the bit breakage, there is an obvious decrement, while in other situations metric entropy nearly remains constant. Owing to metric entropy extraction which is equal to the average value of the plateau where the all dimensions converge in metric entropy graph, a 5% error margin is indicated in variation of metric entropy.
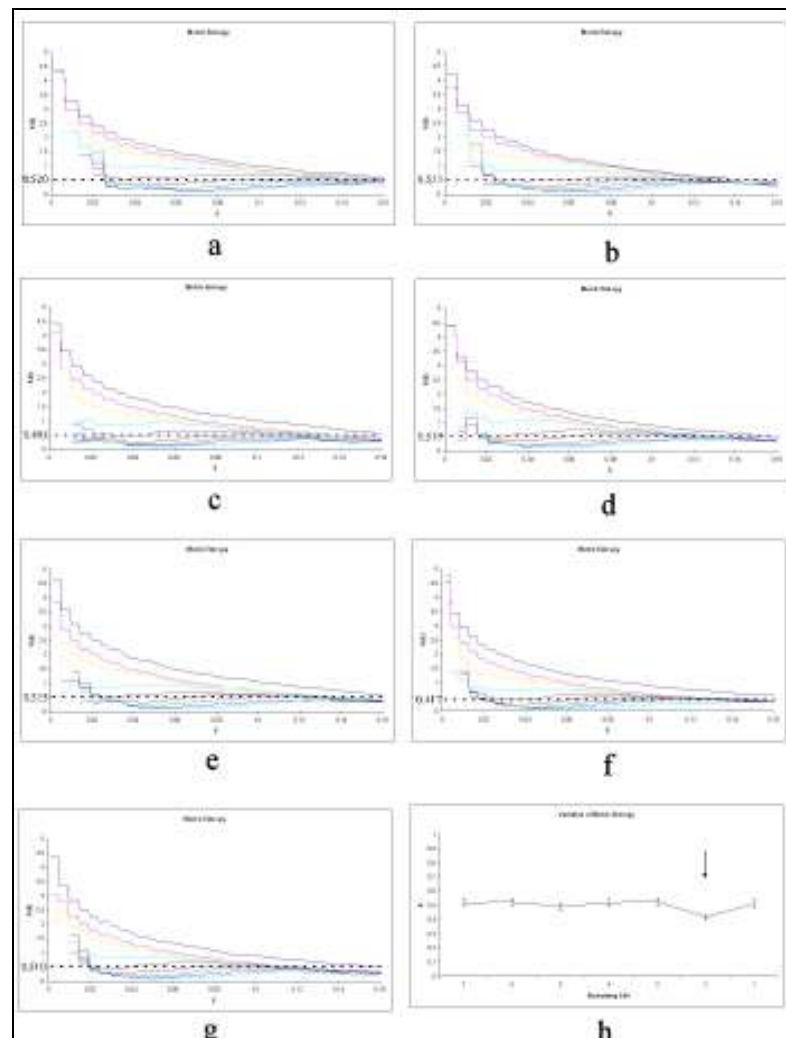

Figure 4.10. (a)-(g) Metric Entropy graph of drill bit 7 (h) Metric entropy variation of drill bit 7
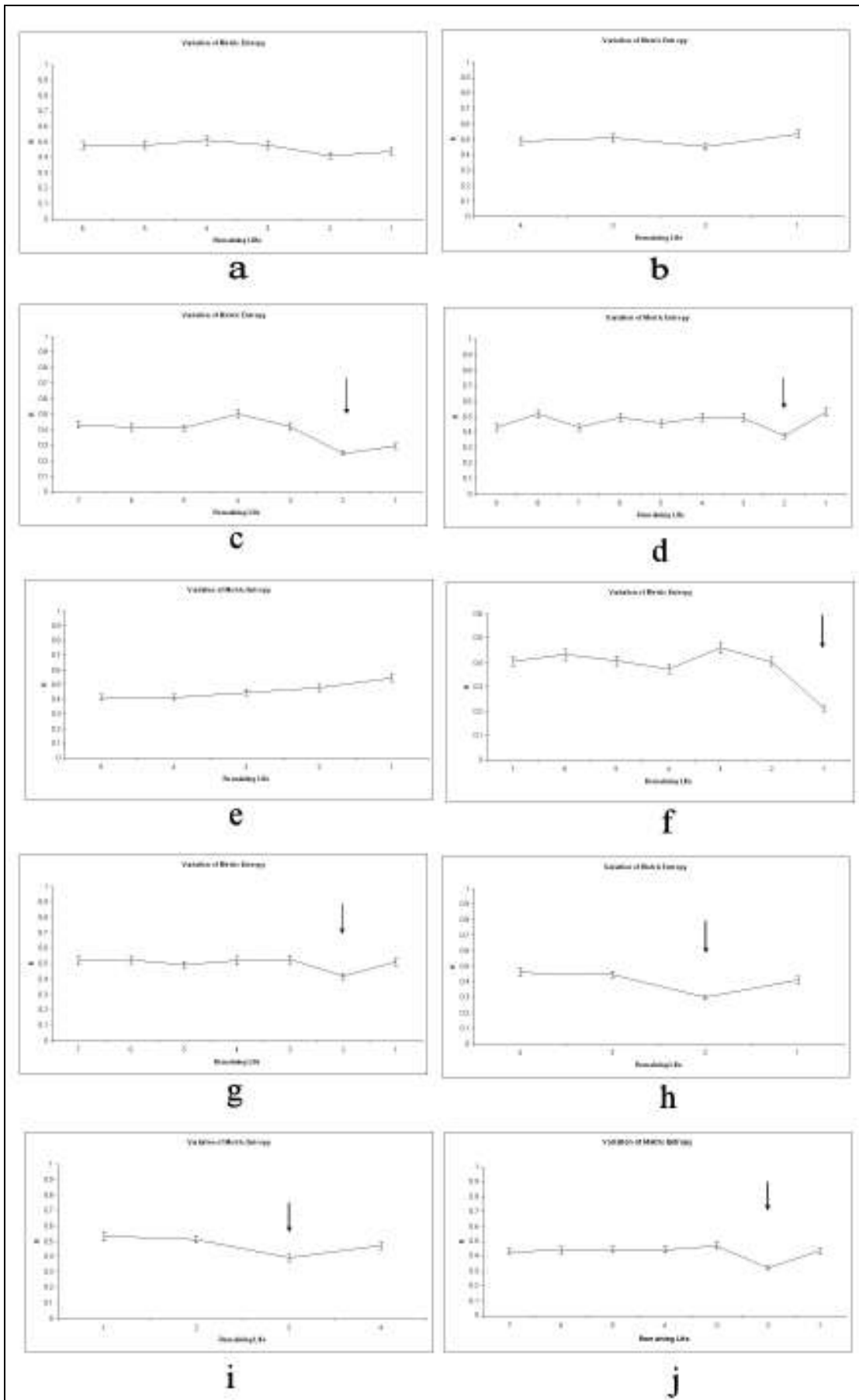
Figure 4.11. (a)-(j) The metric entropy variations of all 10 drill bits 1 to 10.

CHAPTER 5

CONCLUSION

In this study, the prediction of small drill bit breakage by metric entropy was attempted. The vibration signals of the drill were measured in equal time intervals and the nonlinear analysis techniques were applied to the data. Additional to the chaotic invariants, statistical variables were also computed to predict the tool breakage. The experimental results showed that in only variation of metric entropy during the life time of a drill bit, there is a consistent decrement just before the tool breakage. Although the life time variation of the drill bits, which is thought to be caused by the production of drill bits, and the short lifetime of drill bits, the results are promising for a new prognosis technique for mechanical systems. Nonexistence of suitable orientation of the experiment setup during the experiments is a restriction for the reliability of the results.

Finally, with the motivation of promising prediction results, this technique can be applied to the other mechanical systems as an early warning system replacing the unnecessary simple-threshold based warning systems.

For future considerations, making the condition monitoring online in the operation of the selected system, ongoing faults can be detected earlier and the system can be recovered without any failure. Furthermore, this continuous monitoring can be implemented to any system where the early warning system is required.

REFERENCES

Buzug, T. M., 1994. "Characterization of Time Series from Nonlinear Systems", *IEEE Oceans 94 Osates*, Vol. 2, pp. 229-232.

Caputo et al. "Nonlinear Analysis of Experimental Noisy Time Series in Fluidized Bed Systems", *Chaos Solutions and Fractals.*

Chen et al. 1998. "Nonlinear Dynamics of Hourly Ozone Concentrations: Nonparametric Short Term Prediction", *Atmospheric Environment.* Vol. 32, No. 11, pp. 1839-1848.

Craig et al. 2000. "The Use of Correlation Dimension in Condition Monitoring of Systems with Clearance", *Journal of Sound and Vibration 231(1)*, pp. 1-17.

Drongelen et al. 2003. "Seizure Anticipation in Pediatric Epileosy: Use of Kolmogorov Entropy", Pediatric Neurology, Vol. 29, No. 3, pp. 207-213.

Elshorbagy et al. 2002. "Estimation of Missing Streamflow Data Using Principles of Chaos Theory", *Journal of Hydrology 255,* pp.123-133.

Elshorbagy et al. 2002. "Noise Reduction in Chaotic Hydrologic Time Series: Facts and Doubts", *Journal of Hydrology 256*, pp. 147-165.

Govekar et al. 2000. "Analysis of Acoustic Emission Signals and Monitoring of Machining Processes", *Ultrasonics 38,* pp. 598-603.

Grassberger, P., Procaccia, I., 1983. "Estimation of the Kolmogorov Entropy from a Chaotic Signal", *Physical Review A*. Vol. 28, No. 4, pp. 2591-2593.

Hegger et al. 1999. "Practical implementation of Nonlinear time series methods: the TISEAN package", *Chaos 9,* pp. 413-440.

Heng, R.B.W., Nor, M.J.M., 1998. "Statistical Analysis of Sound and Vibration Signals for Monitoring Rolling Element Bearing Condition", *Applied Acoustics*, Vol. 53, No. 1-3, pp. 211-226

Hilborn, R.C., 2000. "Chaos and Nonlinear Dynamics", (Oxford University press).

Kantz, H., Schreiber, T., 1997. "Nonlinear Time Series Analysis", (Cambridge University Press).

Logan, D., Mathew, J., 1996. "Using the Correlation Dimension for Vibration Fault Diagnosis of Rolling Element Bearing – I. Basic Concepts", *Mechanical Systems and Signal Processing*, Vol. 10, No. 3, pp. 241-250.

Logan, D., Mathew, J., 1996. "Using the Correlation Dimension for Vibration Fault Diagnosis of Rolling Element Bearing – II. Selection of Experimental Parameters", *Mechanical Systems and Signal Processing*, Vol. 10, No. 3, pp. 251-264.

Mori et al. 1999. "Prediction of Small Drill Bit Breakage by Wavelet Transforms and Linear Discriminant Functions", *International Journal of Machine Tools & Manufacture*, Vol. 39, pp. 1471-1484.

Pan et al. 1998. "Intelligent Joint Fault Diagnosis of Industrial Robots", *Mechanical Systems and Signal Processing,* Vol. 12, No. 4, pp. 571-588.

Pravitha et al. 2002. "Dynamical aspects of coupled Rossler systems: effects of noise", *Physics Letters A*, Vol. 294, pp. 37-46.

Redealli, S., Macek, W.M., 2001. "Lyapunov Exponent and Entropy of the Solar Wind Flow", *Planetary and Space Science 49,* pp. 1211-1218.

Schreiber, T., Schmitz, A., 2000. "Surrogate Time Series", *Physica D: Nonlinear Phenomena*. Vol. 142, Issues 3-4, pp. 346-382.

Sprott, J.C., 2003. "Chaos and Time Series Analysis", (Oxford University press).

Stark, J. "Analysis of Time Series", *Centre for Nonlinear Dynamics and its Applications*, University Collage London.

Subrahmanyam, M., Sujatha, C., 1997. "Using neural networks for the Diagnosis of Localized Defects in Ball Bearings", *Tribology International*, Vol. 30, No. 10, pp. 739-752.

Tjahjowidodo et al. 2005. "Quantifying chaotic responses of mechanical systems with backlash component", *Article in Press.*

Trendafilova, I., Van Brussel, H., 2001. "Non-linear Dynamics Tools for the Motion Analysis and Condition Monitoring of Robot Joints", *Mechanical Systems and Signal Processing*, Vol. 15, No. 6, pp. 1141-1164.

Xiaoli, L., 1999. "On-line Detection of the Breakage of Small Diameter Drills using current signature Wavelet Transform", *International Journal of Machine Tools & Manufacture*, Vol. 39, pp. 157-164.

APPENDIX A

COMMON CHAOTIC SYSTEMS
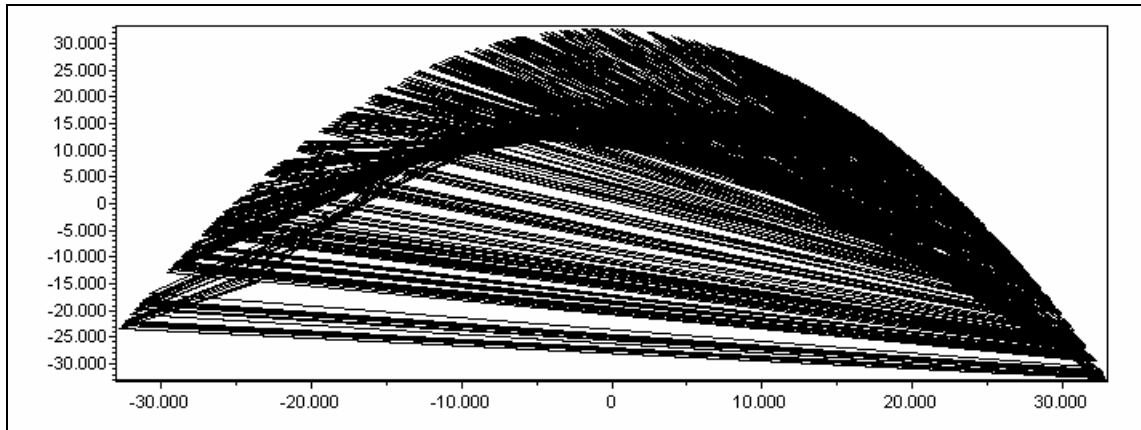

Figure A.1. Phase Portrait of Henon Map

Henon map

$$x_{n+1} = 1 - ax_n^2 + by_n^2$$

$$y_{n+1} = x_n$$

$$a = 1.4, b = 0.3$$

$$x(0) = 0, y(0) = 0.9$$

$$\lambda \cong 0.41922, -1.62319$$
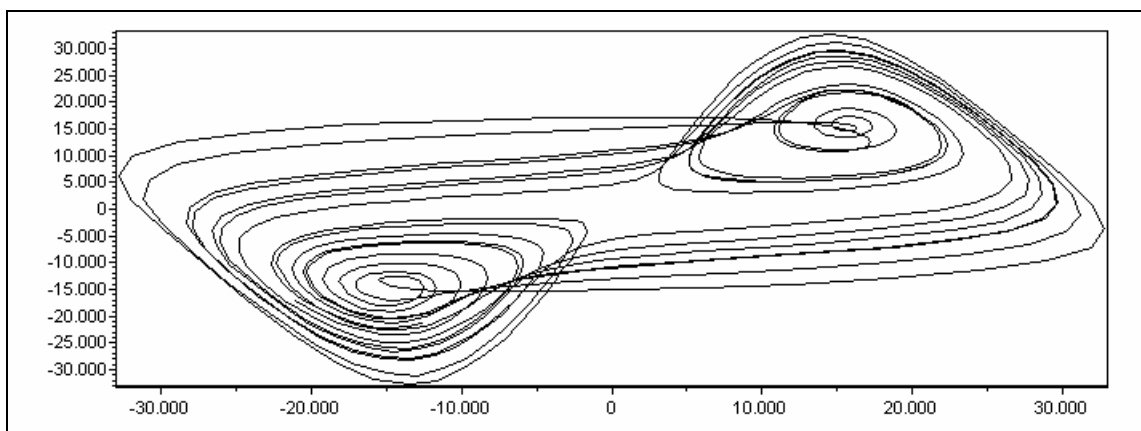
$$D = 1.220$$

(Sprott 2003)

Figure A.2. Phase Portrait of Lorenz Attractor

Lorenz Attractor

$$\dot{x} = \sigma(y - x)$$

$$\dot{y} = -xz + rx - y$$

$$\dot{z} = xy - bz$$

$$\sigma = 10, r = 28, b = 8/3$$

$$x(0) = 0, y(0) = -0.01, z(0) = 9$$

$$\lambda \cong 0.9056, 0, -14.5723$$

$$D = 2.068 \pm 0.086$$

(Sprott 2003)
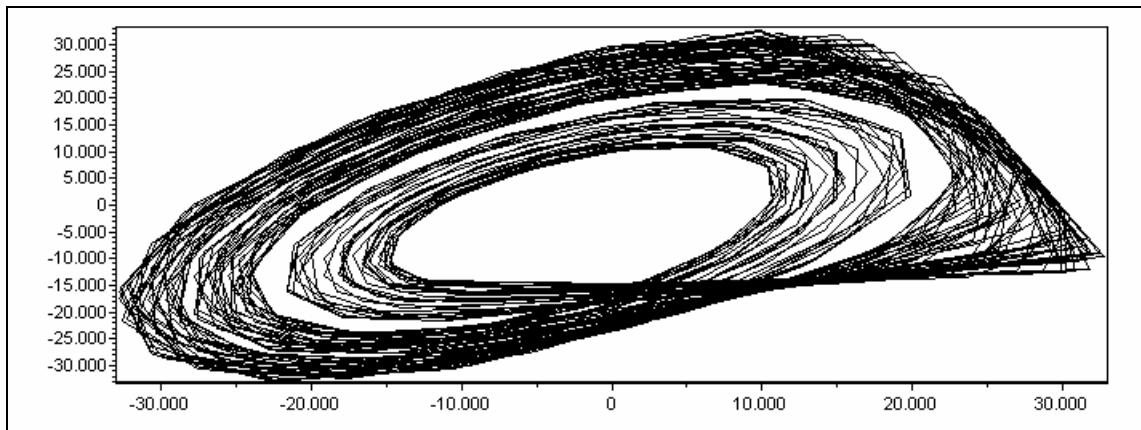
Figure A.3. Phase Portrait of Rössler Attractor

Rössler Attractor

$$\dot{x} = -y - z$$

$$\dot{y} = x + ay$$

$$\dot{z} = b + z(x - c)$$

$$a = b = 0.2, c = 5.7$$

$$x(0) = -9, y(0) = 0, z(0) = 0$$

$$\lambda \cong 0.0714, 0, -5.3943$$

$$D = 1.991 \pm 0.065$$

(Sprott 2003)

APPENDIX B

STATISTICAL PARAMETERS

Root mean square (RMS)

Root mean square indicates the magnitude of variation of a series of discerete values or a continuously varying function. The name comes from the process of RMS. Firstly, the squares the values is taken. Then, mean of the squared values is found. And finally, root of mean of the squared values is calculated.

$$\text{RMS} = \sqrt{\frac{1}{N} \sum_{i=1}^{N} x_i^2} \qquad (B.1)$$

Skewness

Asymmetry in the distribution of the sample data values is called skewness. There are two different tails of the distribution such as left tail having lower value of the distribution and right tail having higher value of the distribution. If the left tail is longer, then the function has negative skewness or left-skewed. On the other hand, if the right tail is longer, then it has positive skewness or right-skewed. Generally, positive skewness is more common than negative skewness.

$$\text{Skew} = \frac{\frac{1}{N} \sum_{i=1}^{N} (x_i - \bar{x})^3}{(\frac{1}{N})^{3/2} (\sum (x_i - \bar{x})^2)^{3/2}} \qquad (B.2)$$

Kurtosis

If the sampled data is skewed, transformation can be applied to the data, for example, taking logarithms of right-skewed data. Then, one can characterize the shape of a distribution by using Kurtosis. If the tails are heavier then for a normal distribution, then Kurtosis of the distribution is positive. Kurtosis of the distribution is negative when the tail are lighter. Kurtosis of zero is possible for the normal distribution.

$$\text{Kurtosis} = \frac{\frac{1}{N} \sum_{i=1}^{N} (x_i - \bar{x})^4}{(\frac{1}{N})^2 (\sum (x_i - \bar{x})^2)^2} \tag{B.3}$$

Crest factor

The Crest factor shows the ratio of the peak value of a waveform to its RMS value . It is defined by a pure number without units. For example, the crest factor of a sine wave is 1.414 when the peak value is 1.414 times the RMS value. A typical vibration signals from an unbalanced machine without any other problems have a nearly 1.5 crest factor. But when the bearings begin to wear, and impacting begins, the crest factor becomes much greater than this. The crest factor is so sensitive to the sharp peaks in the waveform. The reason of this is that the peaks happens suddenly, and hence it does not contain very much energy.

$$\text{Crest Factor} = \left[\frac{\max peak}{RMS} \right] \tag{B.4}$$

APPENDIX C

CULPERTUS

Culpertus is a time series analyzing program which allows time series invariants calculations and graphical representations. Culpertus takes its name from Latin letters "*cul*pa com*pertus*" which means fault certain. Autocorrelation, correlation sum, correlation dimension and metric entropy can be calculated with Culpertus. To download culpertus, please visit *http://www.iyte.edu.tr/~erhansevil/*
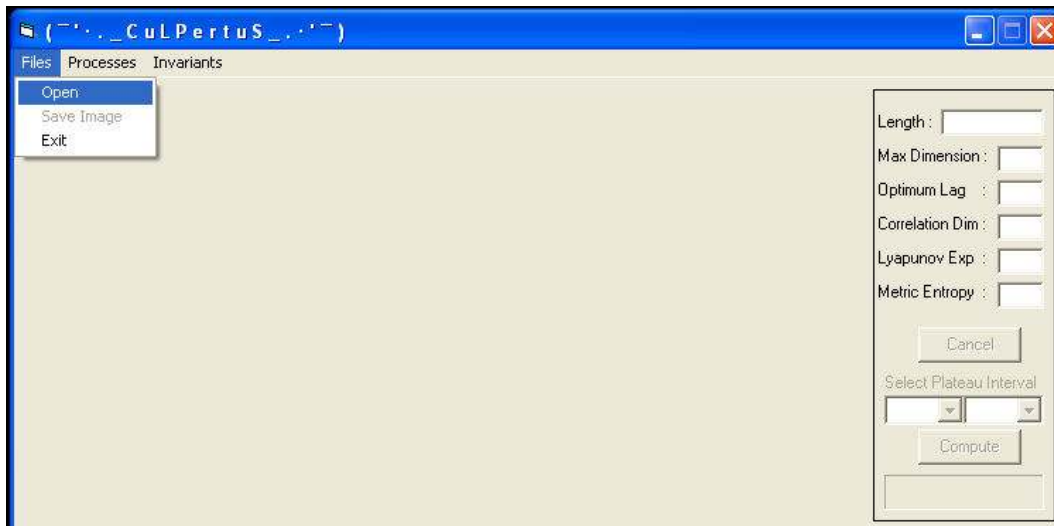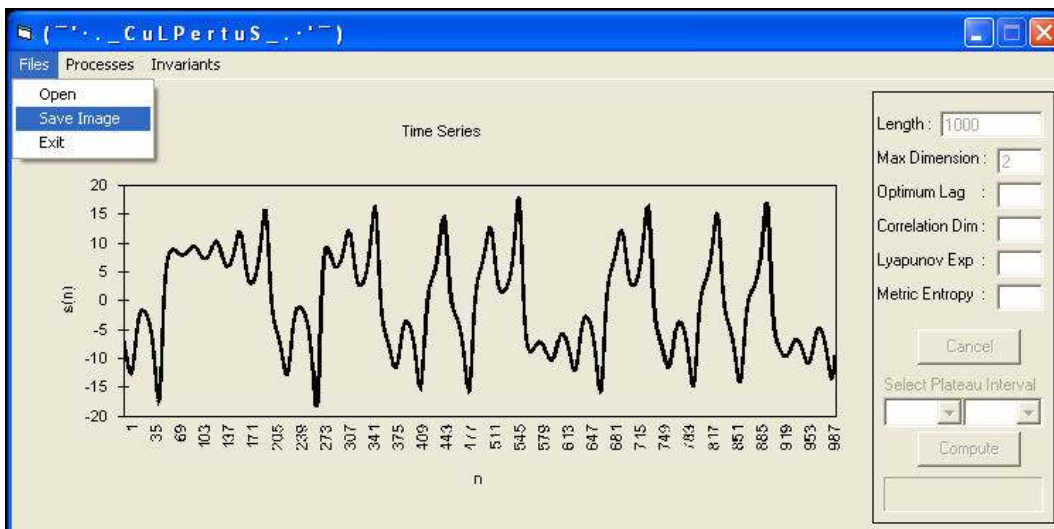

Figure C.1. Culpertus Open file

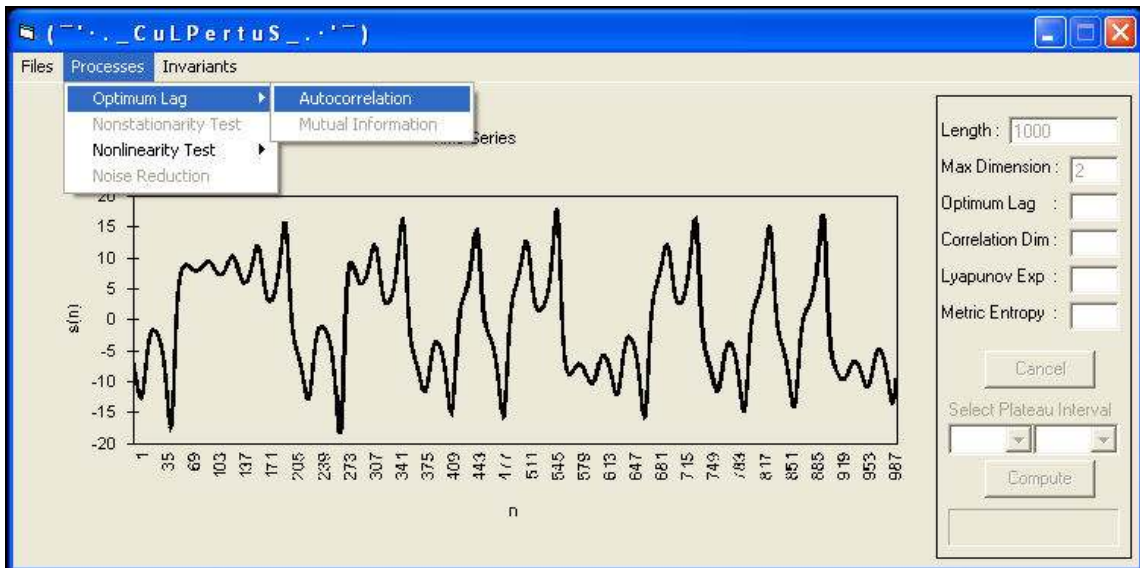Figure C.2. Culpertus Save Image

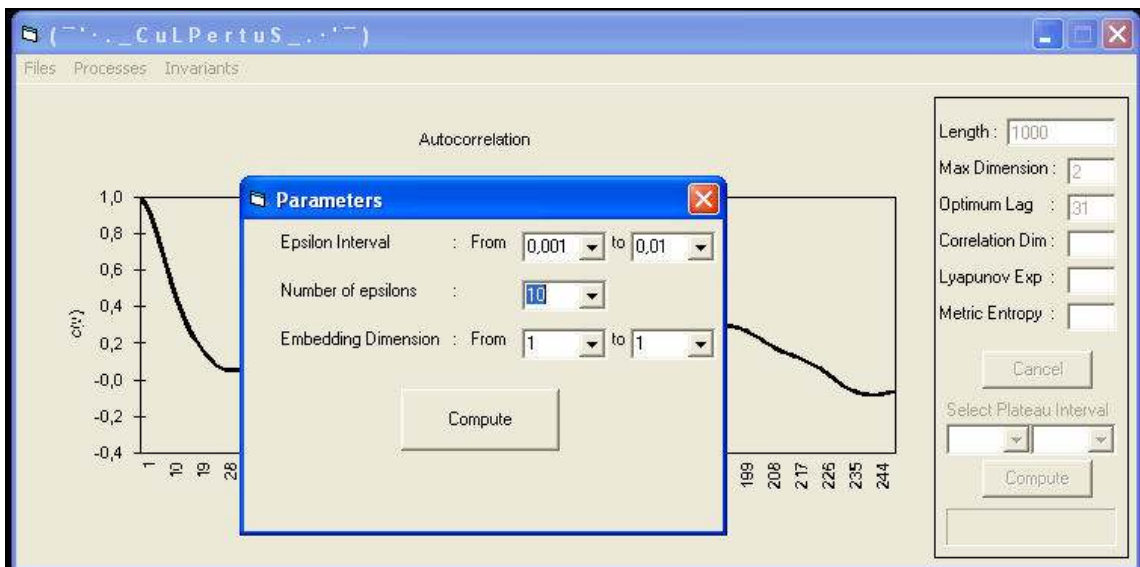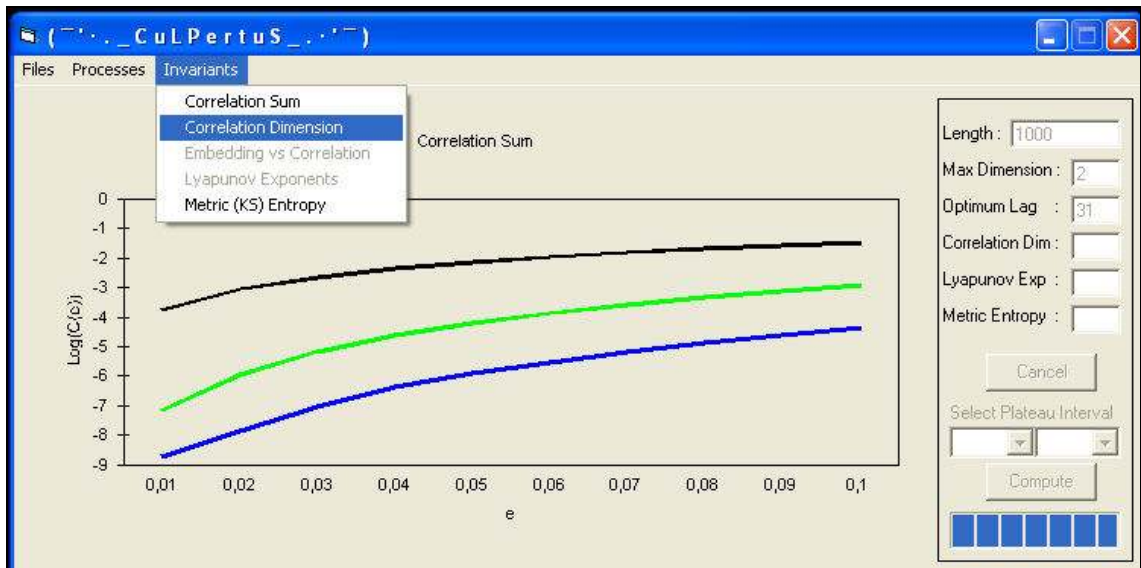Figure C.3. Culpertus Autocorrelation

Figure C.4. Culpertus Correlation Sum Parameters

Figure C.5. Culpertus Chaotic Invariants